AN ABSTRACT OF THE THESIS OF

SIAMAK HASSANZADEH for the degree of MASTER OF SCIENCE

in GEOPHYSICS presented on February 9, 1976

Title: DETERMINATION OF DEPTH TO THE MAGNETIC BASEMENT USING MAXIMUM ENTROPY WITH APPLICATION TO THE NORTHERN CHILE TRENCH

Redacted for Privacy

Abstract approved: _____
Dr. Richard J. Blakely

Power spectral analysis using the maximum entropy method is applied to the estimation of depth to the source of magnetic anomalies. The method assumes that the source is two-dimensional and has a magnetization with random intensity. The predictive ability of the maximum entropy technique permits analysis of short segments of data in order to resolve short wavelength variations in source depth. The method does not require knowledge of susceptibilities or the magnetic declination and inclination. An application of the method to theoretical data and observed marine anomalies over the Peru-Chile trench yields encouraging results. Specifically, for the eastern margin of the Nazca plate, analyses generally indicate a continuous magnetic basement extending into the subduction zone. The basement is shallow seaward of the trench axis and deepens as the plate approaches the convergent margin. This apparent deepening is postulated to be due to the

thickening of the oceanic crust and the deterioration of its magnetization, possibly caused by the compressional disruption of the basaltic layer. Landward of the trench axis, the depth estimates indicate possible uplift of the oceanic material into the lower slope of the continental margin.

Determination of Depth to the Magnetic Basement Using Maximum Entropy with Application to the Northern Chile Trench

by

Siamak Hassanzadeh

A THESIS

submitted to

Oregon State University

in partial fulfillment of
the requirements for the
degree of

Master of Science

Completed February 1976

Commencement June 1976

APPROVED:

Redacted for Privacy

Assistant Professor of Geophysics
in charge of major

Redacted for Privacy

Dean of School of Oceanography

Redacted for Privacy

Dean of Graduate School

Date thesis is presented February 9, 1976

Typed by Clover Redfern for Siamak Hassanzadeh

ACKNOWLEDGMENTS

I would like to extend my deepest appreciation to Dr. Richard Blakely for his advice, assistance, and encouragement during the past year. Particularly, I would like to thank him for critically reading the manuscript as the preparation of the thesis would not have been possible without his comments and criticisms.

Discussions with William Schweller were of great help in interpretation of the results from the Chile trench.

I would also like to thank Dr. Richard Couch, Dr. LaVerne Kulm, Jonathan Hanson, Paul Jones, and Glenn Thrasher for their help and suggestions on the manuscript.

I am also grateful to Janet Gemperle and Jack Weisman for drafting the figures, and to Judy Keser for proofreading the manuscript.

This research was conducted within the framework of the Nazca Plate Project and was supported through the National Science Foundation, International Decade of Ocean Exploration (Grant GX-28675).

TABLE OF CONTENTS

LIST OF FIGURES

DETERMINATION OF DEPTH TO THE MAGNETIC BASEMENT USING MAXIMUM ENTROPY WITH APPLICATION TO THE NORTHERN CHILE TRENCH

INTRODUCTION

Automated techniques for the determination of depths to magnetic sources have been developed extensively in recent years. These techniques generally involve magnetic profiles but differ, depending on the assumed source. Deterministic techniques (Nabighian, 1972, 1974) assume two dimensional prismatic sources of polygonal cross section with uniform magnetization. An analytic function is generated whose real part is the horizontal derivative of the field profile and whose imaginary part is the vertical derivative. Such a function consists of a finite number of simple anomalies corresponding to the corners of the polygons. The locations of these corners are determined with operations on the analytic function. This model is also used in iterative techniques which attempt to fit the observed magnetic profile by automated adjustment of assumed source configurations. Statistical techniques, on the other hand, assume sources of random intensity distributed over two dimensional surfaces at depth.

Although the latter approach cannot be expected to have the resolution theoretically achievable by analysis carried out on individual anomalies, it can lead to the determination of reasonable

depth values to major units of magnetic sources. In particular, the statistical approach may sometimes be preferable, because more than one anomaly can then be used to determine depths to magnetic structures. Also, the inevitability of noise resulting from the acquisition process makes the analyses of individual anomalies less reliable for all practical concerns. Types of noise include navigational errors and external sources (e.g., diurnal variations and magnetic storms). Noise can also arise from geological sources such as shallow interbedded sediments and volcanics overlying a deeper crystalline basement. The shallow sources contribute a high wavenumber noise component to the basement anomaly.

Serson and Hannaford (1957) first used a statistical approach to determine the source depth. They calculated the theoretical autocorrelation function of the total field anomaly assuming there is an uncorrelated distribution (see Appendix I) of monopoles and vertical dipoles at some distance z below the observation line. The source depth z is then simply obtained from the autocorrelation function by (Phillips, 1975)

$$z = \frac{x}{2} \sqrt{\frac{1}{1/\phi(x) - 1}} \qquad (1)$$

where z is the depth to the top of the magnetic source, and $\phi(x)$ is the normalized autocorrelation function. Recent studies (Gudmundsson, 1966; Bhattacharyya, 1966) indicate that the power

spectrum is simply related to source depth. Spector and Grant (1970) developed a depth-determination method which matches two-dimensional power spectra of observed data with corresponding spectra obtained from a theoretical model. Their model assumes that an uncorrelated distribution of magnetic sources exists at a number of discrete depth intervals in the geologic column.

The approach of Spector and Grant (1970) requires the availability of gridded magnetic data, from which two-dimensional power spectra are computed for depth analysis. These spectra are also functions of the magnetic inclination and declination. Treitel and others (1971) developed a depth determination technique which utilizes single profiles. They assume that there is a single uncorrelated distribution of infinitely long magnetic line sources at a depth z below the profile of observation and that these line sources approximate the effect of a magnetically susceptible basement overlain by layers of sedimentary rocks. Their approach is independent of the magnetic declination and inclination.

Unfortunately, statistical techniques are used primarily to obtain source parameters averaged over large regions. This restriction has been largely due to the poor response of the conventional autocorrelation or power spectral estimators in the presence of highly non-stationary data. Phillips (1975) suggested the use of an unconventional estimation method which provides reliable autocorrelation

coefficients from very short data sets. This is the maximum entropy method developed by Burg (1967, 1968). By using an adaptive approach to obtain maximum entropy autocorrelation coefficients, Phillips was able to achieve source resolution comparable to that of non-statistical techniques.

In this paper we extend the method of Treitel and others (1971) by using maximum entropy to estimate power spectra. To these estimated spectra, we fit theoretical spectra which depend on the depth to the magnetic source. Because of the predictive ability of maximum entropy, short segments of data can be used for each depth calculation so that the method presented here can resolve short wavelength changes in source depth.

We shall begin by developing the mathematical basis of the new method. Then we shall apply the present technique to a set of theoretical and observed magnetic intensity data and compare results obtained with the new method with results from Phillips' technique. The observed profiles are from recent surveys of the Peru-Chile Trench.

THEORY

We shall assume that the magnetic source is two dimensional and represented by a horizontal layer of finite thickness, extending infinitely in the x and y directions (Figure 1). Further, we shall assume that the profile is measured in the x direction and that x is perpendicular to the strike of the structure. Inside the layer the magnetic intensity of the model is allowed to vary only with x.

The observed magnetic anomaly profile $h(x)$ for such a model can be represented by the superposition of anomalies produced by horizontal planar sources within the layer. If we consider a horizontal element with infinitesimal thickness dw (see Figure 2), then $h(x)$ can be expressed as

$$h(x) = \int_{z}^{z+t} h_w(x)dw \qquad (2)$$

where $h_w(x)$ is the magnetic anomaly due to a planar source at depth w, z is the depth to the top of the layer, and t is the thickness of the layer. The magnetic anomaly for a magnetized plane is given by the convolution of the magnetization $m(x)$ with the impulse response of the plane $g_w(x)$ (Blakely and Cox, 1972), i.e.,

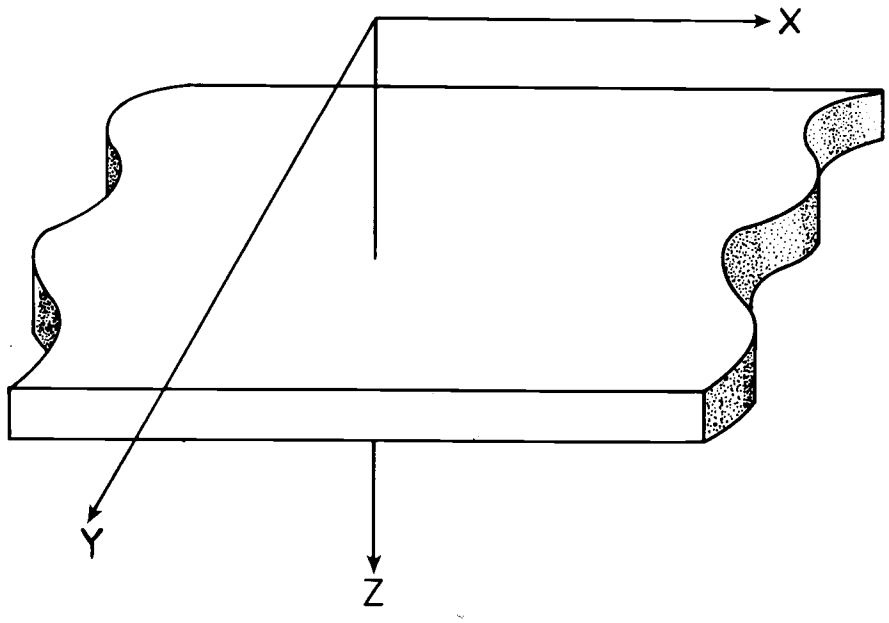

Figure 1. The schematic representation of a two-dimensional horizontal layer of infinite extent in the x and y dimensions.

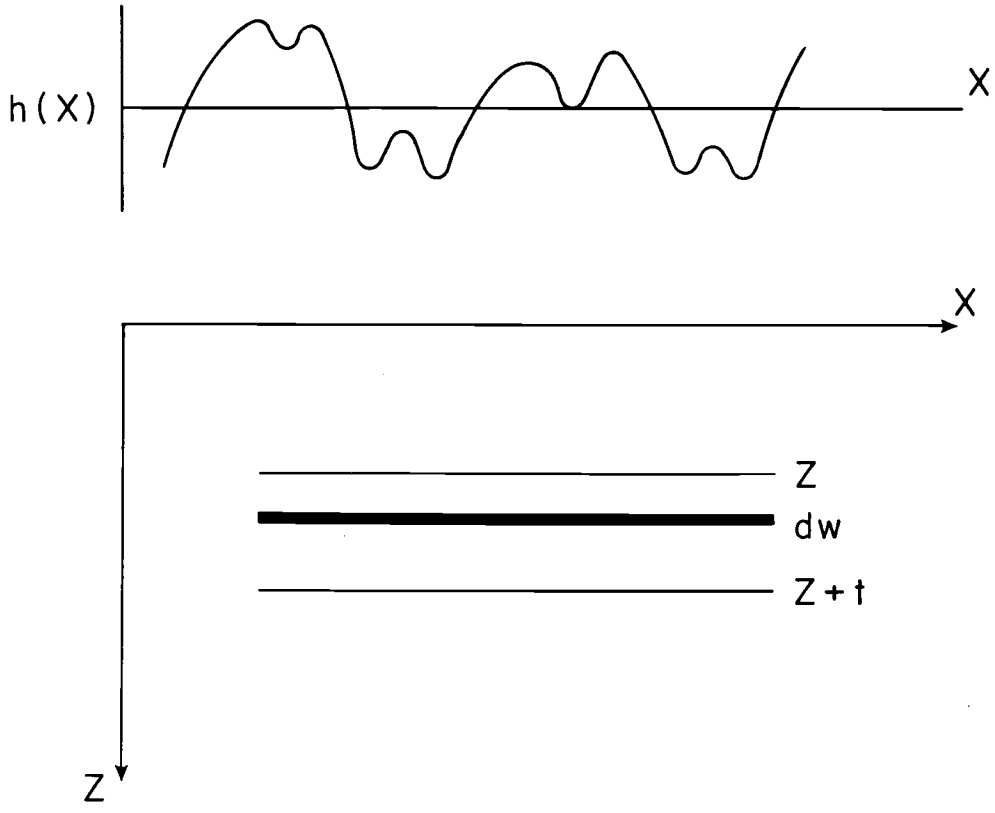

Figure 2. The spatial geometry for deriving the total field anomaly h(x) produced by the model in Figure 1. h(x) can be represented by the superposition of anomalies produced by horizontal planar sources of thickness dw within the layer.

$$h_w(x) = \int_{-\infty}^{+\infty} m(u) g_w(x-u) du \ . \qquad (3)$$

Combining Equations (2) and (3), we obtain

$$h(x) = \int_{z}^{z+t} \int_{-\infty}^{+\infty} m(u) g_w(x-u) du dw \ . \qquad (4)$$

Applying the Fourier convolution theorem, that two functions convolved in the space domain and two functions multiplied in the wavenumber domain are transform pairs, and assuming that the Fourier transforms of $h(x)$, $m(x)$, and $g_w(x)$ exist, we arrive at

$$H(k) = \int_{z}^{z+t} M(k) G_w(k) dw \qquad (5)$$

where $H(k)$, $M(k)$, and $G_w(k)$ are the Fourier transforms of $h(x)$, $m(x)$, and $g_w(x)$, respectively and where k is the wavenumber in the x direction. Since the magnetization is invariant in the vertical direction, Equation (5) can be rewritten as

$$H(k) = M(k) G(k) \qquad (6)$$

and where

$$G(k) = \int_{z}^{z+t} G_w(k) dw \qquad (7)$$

is the wavenumber response of a horizontal layer. Notice that $G(k)$ is a function of the depth to the top of the layer.

The power spectrum of the magnetic intensity can be obtained by squaring its Fourier amplitude spectrum. If we let $P(k)$ be the power spectrum of $h(x)$, it can be expressed by

$$P(k) = |H(k)|^2 = |M(k)|^2 |G(k)|^2 \tag{8}$$

In general, the power spectrum of the magnetic source $|M(k)|^2$ is not known. We shall assume, therefore, that the magnetic distribution $m(x)$ is uncorrelated (see Appendix I) so that its power spectrum is a constant, say C. Hence, Equation (8) becomes

$$P(k) = C|G(k)|^2 \tag{9}$$

The assumption of uncorrelated magnetization is not unreasonable. Observation of remanent magnetic directions and intensities have indicated a certain degree of randomness, even when measured along the same stratigraphic horizon (Phillips, 1975). Also, a recent study by Puranen and others (1968) over a 1200 square-kilometer exposed shield area in Finland has shown that the measured susceptibility values of some 4700 samples of igneous rock follows a roughly log-normal distribution.

To complete the development of the basic relation (9), we require an expression for $G(k)$.

Wavenumber Response of a Horizontal Layer

In order to derive an expression for $G(k)$ we must obtain $G_w(k)$, the wavenumber response of a horizontal plane. To aid in this derivation, we define the following notation:

I, D	Inclination and declination of the regional magnetic field.
I_m, D_m	Inclination and declination of the source magnetization.
S	Azimuth of the strike of the magnetic body.

It is convenient to introduce notations for the effective inclinations I' and I'_m

$$I' = \tan^{-1}\left[\frac{\sin I}{\cos I \sin(S-D)}\right]$$
$$I'_m = \tan^{-1}\left[\frac{\sin I_m}{\cos I_m \sin(S-D_m)}\right] \qquad (10)$$

and for the effective magnitudes F' and M'

$$F' = \frac{\sin I}{\sin I'}$$
$$M' = \frac{\sin I_m}{\sin I'_m} \qquad (11)$$

Effective inclinations and magnitudes are those observed after projecting the regional field vector and magnetization vector onto a

plane perpendicular to the strike of the source.

The wavenumber response of a horizontal magnetic sheet at depth w is given by Blakely and Cox (1972)

$$G_w(k) = -2\pi|k|F'M'e^{-w|k|}(\cos B - i \operatorname{sgn} k \sin B) \qquad (12)$$

where $B = I' + I'_m$, and where $\operatorname{sgn} k$ is the sign function defined by (Bracewell, 1965, pp. 61-62)

$$\operatorname{sgn} k = \begin{cases} -1 & k < 0 \\ +1 & k > 0 \end{cases}$$

Substituting expression (12) for $G_w(k)$ in (7) and carrying out the integration we obtain

$$G(k) = -2\pi F'M'(\cos B - i \operatorname{sgn} k \sin B)(e^{-z|k|} - e^{-(z+t)|k|}) \qquad (13)$$

Equation (13) is the wavenumber response of a horizontal layer.

Depth Formula

Substituting Equations (13) into Equation (9) yields

$$P(k) = Ae^{-2z|k|}(1-e^{-t|k|})^2 \qquad (14)$$

where $A = 4\pi^2F'^2M'^2C$. Equation (14) depends on the depth to the magnetic layer z and thus provides a means of estimating the

source-depth from a measured profile. Since the estimation of the empirical spectrum is generally done digitally, it is appropriate to express Equation (14) for digitized profiles. Let such a profile be represented by a series of N equispaced magnetic intensity values $h_i = (h_1, h_2, \ldots, h_N)$, and let the uniform sampling increment be Δx. The power spectrum will then be estimated at the sequence of wavenumbers k_i given by

$$k_i = \frac{\pi i}{M \Delta x}, \quad i = 0, 1, \ldots, M \tag{15}$$

where $k_M = \pi$ radians/sampling increment is the Nyquist wavenumber (Blackman and Tukey, 1959, p. 32). The digital representation of Equation (14) is then

$$P_i = A e^{-2zk_i} (1 - e^{-tk_i})^2 \tag{16}$$

Taking the natural logarithm of both sides of (16) yields

$$\ln P_i = \ln A - 2zk_i + 2 \ln(1 - e^{-tk_i}) \tag{17}$$

There are three unknowns in Equation (17): A, z, and t. Since the number of field points M is generally much larger than three, the problem is over-determined (i.e., there are more equations than unknowns). The problem is, however, much simpler

if we treat t as a known parameter. Then, rearranging (17) leads to a set of $M+1$ equations and two unknowns, i.e.,

$$\ln A - 2k_i z = \ln P_i - 2\ln(1-e^{-tk_i}), \quad i = 0, 1, \ldots, M \tag{18}$$

A solution for z can be obtained using the least square method and the details of the derivation are given in Appendix II. The final expression for z is

$$z = \frac{\sum_{i=0}^{M} c_i \sum_{i=0}^{M} k_i - M \sum_{i=0}^{M} k_i c_i}{M \sum_{i=0}^{M} k_i^2 - \left(\sum_{i=0}^{M} k_i \right)^2} \tag{19}$$

where $c_i = (1/2) \ln P_i - \ln(1-e^{-tk_i})$.

The range of values for the depth extent t of a given source is restricted by a number of geological and geophysical considerations. For example, the Curie temperature of most rocks is reached by a depth of several tens of kilometers, thus placing an upper limit on t. Also, studies on the magnetization of oceanic crust indicate that the major portion of magnetization is due to magnetic materials confined to an even thinner layer, on the order of 500 meters (Bott, 1967; Parker and Huestis, 1974; Talwani and others, 1971). For other applications, if the majority of the bodies in an area extend to

such depths that their bottoms cannot be discerned clearly through the observation window (i.e., the survey gate), t becomes so large that the second term on the right of Equation (18) becomes negligible, thus reducing (18) to

$$\ln A - 2k_i z = \ln P_i, \quad i = 0, 1, \ldots, M \tag{20}$$

For this special case a plot of $\ln P_i$ versus k_i is a straight line with slope equal to $-2z$.

Equation (19), applied to power spectra estimated from anomaly profiles, provides a means of determining the depth to the layer. In finding power spectra, it is desirable to use the smallest possible number of data points in order to maximize resolution, and maximum entropy fulfills this requirement.

MAXIMUM ENTROPY SPECTRAL ESTIMATION METHOD

Until recently, more conventional spectral estimation methods were based on the approach of Blackman and Tukey (1959). In this approach, the samples of the autocorrelation function are estimated from the data, weighted, and Fourier transformed to obtain an estimate of the power spectrum. The introduction of the Fast Fourier Transform (FFT) (Cooley and Tukey, 1965) has made estimation methods based on the periodogram (Jones, 1965) more popular. These direct methods estimate the spectrum, using the squared magnitude of the transform of time-series data. Either the magnitude squared is averaged for different samples of data or the magnitude squared is smoothed in the frequency domain to get a stable estimate of the spectrum.

All of the usual methods of spectral analysis make rather unrealistic assumptions about the extension of the data outside the known interval: the Blackman and Tukey approach assumes a zero extension to the data, whereas the periodogram assumes a periodic extension. Also, these methods require window functions which are independent of the data or the properties of the random process which is analyzed. This window function relates the average estimated spectrum to the true spectrum. One main difficulty with these methods is that the window does not depend upon the true spectrum.

Another problem, particular for this study, is the gate-length (i.e., the sample length used in estimating the power spectrum). In estimating the change in the power spectrum of a long series of non-stationary data, we would like to make the gate-length as short as possible in order to detect short wavelength changes in the spectral quality of the data. On the other hand, better spectral estimates are found with long gate-lengths. We are thus faced with a trade-off between high resolution and good spectral estimates. Restrictions due to the poor response of conventional power spectral estimators, as mentioned earlier, have resulted in determination of values averaged over large regions. Specifically, previous attempts to determine depths to magnetic sources from isolated profiles have yielded a 'single' value for an entire length of the magnetic profile (Treitel and others, 1971). Hence, undulations of the basement surface having periods equal to or less than the profile length could not be detected.

A new method, the maximum entropy method (MEM) developed by Burg (1967, 1968), has considerable advantages over the usual methods. Unlike conventional methods, the MEM does not require a fixed window function, and is especially valuable when the length of available data might be limited. (The amount of data might be limited because phenomena can be considered stationary only over limited intervals of time, or because data can be collected only over a fixed time interval, or both.) Also, in contrast to previous methods,

Burg's method makes no assumption about the extension of data samples. Rather, it generates a unique filter based upon information contained within the available data. This filter, known as the prediction error filter (PEF), if applied to the data, would "whiten" the input data samples, i.e., produce an uncorrelated sequence. Since the spectrum of an uncorrelated series is a constant, the spectrum of the input is proportional to the reciprocal of the power response of the filter.

To illustrate how the MEM operates, consider a discrete time series x_t. From stochastic theory (Kanasewich, 1975, pp. 357, 358), any nondeterministic stationary stochastic process can be represented by a moving summation:

$$x_t = \sum_{s=0}^{\infty} b_s y_{t-s}, \quad b_o = 1 \tag{21}$$

The sequence y_t is white noise with zero mean and variance σ^2. Note that Equation (21) is the convolution of b_t and y_t.

The inverse of the moving average process is the deconvolution

$$y_t = \sum_{i=0}^{\infty} a_i x_{t-i}, \quad a_o = 1 \tag{22}$$

The parameters a_t may be regarded as the coefficients of a whitening filter. Burg (1968, 1970) showed that these coefficients can be computed without requiring either a zero or periodic extension to the data. Qualitatively, this procedure involves minimizing the power output of a finite prediction error filter that is run over the data, but not off the data, in a forward and backward manner. The length of the filter should not exceed that of the time series. More detailed treatments of this procedure have been given by Burg (1970), Ulrych (1972), and Kanasewich (1975).

Once the appropriate filter is determined, the power spectrum of the time series can be estimated using the theorem in time series analysis that the power spectrum of the output from a linear system is obtained by multiplying the power spectrum of the input by the square of the modulus of the frequency response function of the system (Jenkins and Watts, 1968, p. 227). The power spectrum of band-limited white noise is simply the variance of the noise divided by its bandwidth. Hence, if we consider the convolution (21), $P_x(k)$, the power spectrum of x_t, is given by

$$P_x(k) = (\sigma^2 / 2 f_N) \left| B(k) \right|^2 \tag{23}$$

where

$$B(k) = \sum_{s=0}^{\infty} b_s \exp(-2\pi i s k \Delta x), \quad b_o = 1 \tag{24}$$

Δx is the sampling interval, and f_N is the Nyquist frequency = $1/(2\Delta t)$. Since $B(k) = A^{-1}(k)$,

$$P_x(k) = \frac{\sigma^2/2f_N}{|A(k)|^2}$$

or,

$$P_x(k) = \frac{\sigma^2/2f_N}{\left|1+\sum_{n=1}^{\infty} a_n \exp(-2\pi i n k \Delta x)\right|} \tag{25}$$

In practice, $P_x(k)$ is estimated using a finite length of the prediction error filter a_t. It will be shown below that the shape of $P_x(k)$ depends on the number of terms in this filter. More detailed discussions of MEM are given by Lacoss (1971) and Kanasewich (1975).

Previous experiments and applications of the MEM have dealt with random processes containing one or more periodic components which were to be resolved (Lacoss, 1971; Ulrych, 1972; Ulrych and others, 1973; Chen and Stegen, 1974; Denham, 1975). In this paper we will attempt to extend the application of the MEM to a more general type of random process, namely, the magnetic pattern of distant sources in order to determine their depths. Our application of maximum entropy differs from previous work in that the expected spectrum of a magnetic anomaly produced by uncorrelated sources is smooth and without spikes (see Equations (9) and (13)).

TEST OF THE METHOD ON THEORETICAL DATA

The depth determination method was applied to magnetic intensity profiles generated from theoretical models in order to test its accuracy and resolution. The general model employed was a one-kilometer thick, horizontal layer with uncorrelated magnetization. Figure 3 shows some specific spectral estimates of this artificial data using the maximum entropy technique. For each example of Figure 3, the total number of data points is 101 and the sample interval is 2 km. The estimates are for 4-, 10-, 14-, and 18-term prediction error filters, respectively. An unsmoothed spectral estimate obtained by using the Fast Fourier Transform technique is also shown for comparison. The theoretical spectrum was calculated without considering the values of the effective inclination and declination. Their effect would be to shift the spectrum vertically, and hence, no change would be made on the shape of the spectrum. The superiority of the maximum entropy spectral estimates (MESE) relative to the conventional Fourier transform is self evident.

The quality of the MESE, however, varies with the number of terms of the prediction error filter (NPEF). The resolution is relatively poor for short prediction error filters (Figure 3, A). As the number of terms in the filter increases resolution improves but spurious spikes appear (Figure 3, D). For filter lengths of the order of the

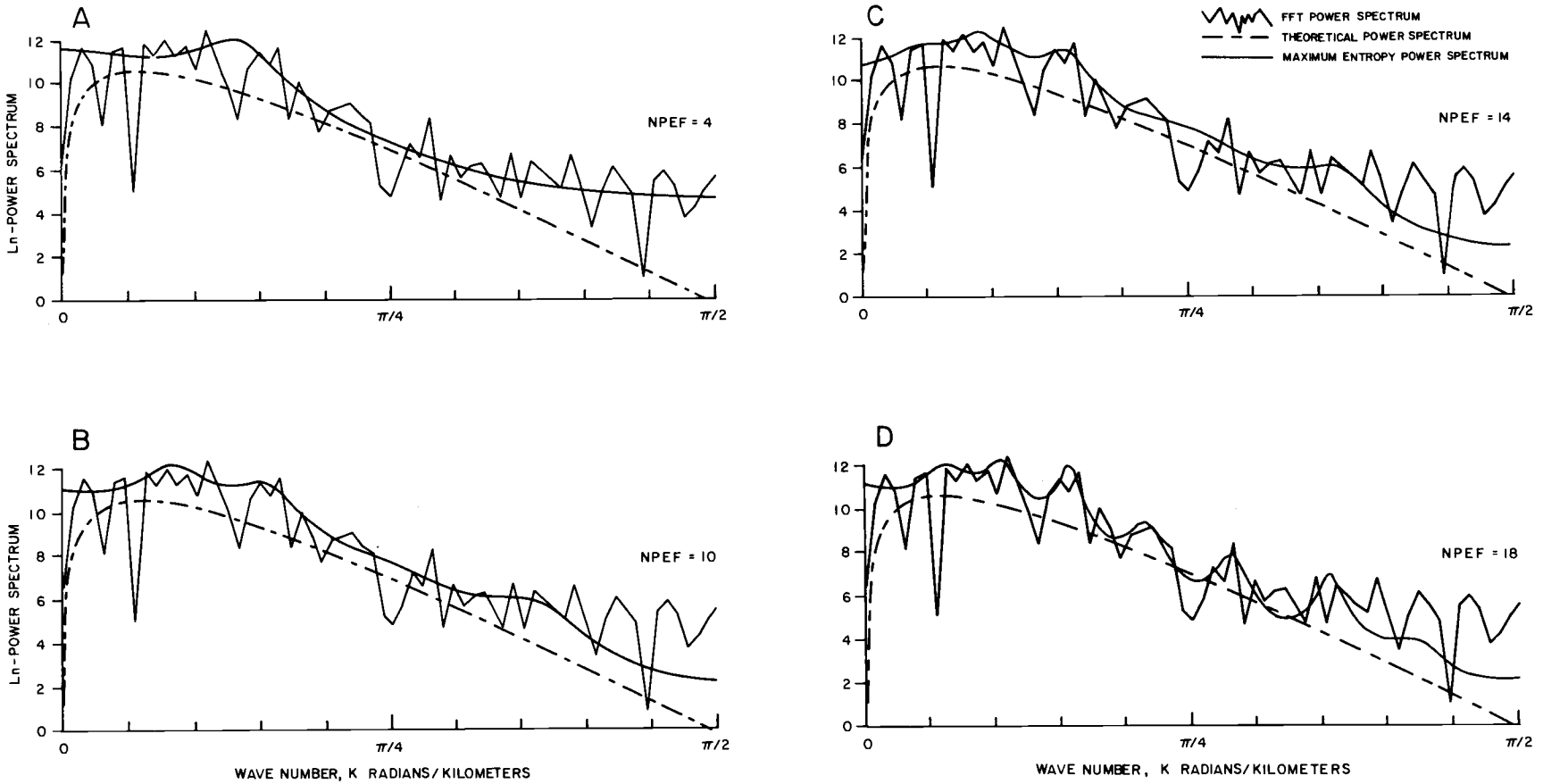

Figure 3. Spectral estimates of theoretical data using maximum entropy method. NPEF is the number of terms in the prediction error filter.

length of the input time series, maximum entropy spectrum approaches that determined with the FFT. Such results have also been observed by other investigators (Chen and Stegen, 1974; Ulrych and Bishop, 1975) who found that too short a length for the filter results in a highly smoothed estimate, obviating the resolution advantages of the MEM, whereas an excessive length introduces artificial detail into the spectrum.

A problem of the MEM is the subjective choice of an optimum length of the prediction error filter. This was recently discussed by Ulrych and Bishop (1975). They applied the statistical work of Akaike (1969, 1970) to the MEM and found that, for predictive deconvolution and spectral estimation, the optimum filter length may be found objectively by monitoring the final prediction error (FPE). This is an estimate of the mean square error in prediction (i.e., the prediction variance) expected when a predictor, calculated from one observation of a process, is applied to an independent observation of the same process. Choosing the filter length for which the FPE is a minimum gives the best mean-square compromist between bias and variance errors in the filter. The filter so obtained is the optimum for spectral estimation. Ulrych and Bishop (1975) found that this criterion works very well with the MEM, but they indicate that not all processes may exhibit a clear minimum in the FPE. For such cases a limit on the length of the prediction error filter of half of the data length must

be imposed. More details are given by Ulrych and Bishop (1975) and Fryer and others (1975). For the analysis of data in this study a filter length of 10 was chosen based on empirical observations since the application of the FPE would be a task beyond the scope of this study.

Another problem with the MESE is that they generally deviate from the theoretical spectrum at very small and very large wavenumbers (see Figure 3). The extent of this deviation also depends on the number of terms of the prediction error filter: being the greatest for the short filter and decreasing with an increase in the length of the filter. It has been observed that the divergence of the estimates from the true spectrum is of greater extent near the Nyquist frequency (wavenumber) than at small wavenumbers. This problem may be alleviated by excluding both ends of the spectral estimates when fitting them to Equation (19). A criterion for such a spectral cutoff would be to omit portions of the spectral estimates at large wavenumbers where estimates fall below a certain percentage, say 1%, of the spectral peak. At small wavenumbers, where the deviation from the theoretical spectrum is less critical, one can generally exclude the portion prior to the observed spectral peak.

The quality of maximum entropy spectrum also depends on the sample length. Figure 4 shows the spectrum of the magnetic profile of Figure 3 obtained using a sample length of 30 data points and a

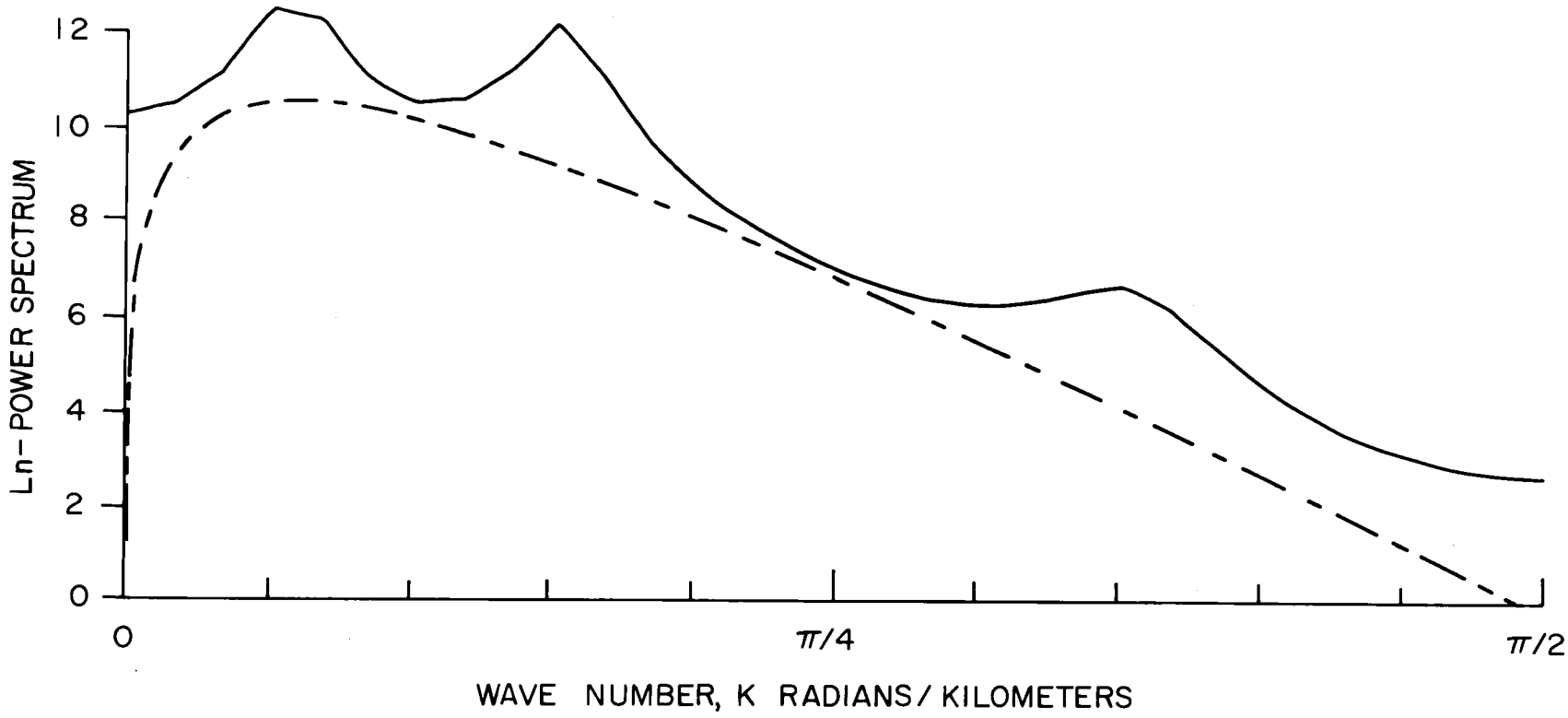

Figure 4. Maximum entropy spectral estimate of the data in Figure 3 for a sample length of 30 data points. Broken line represents the theoretical spectrum. NPEF = 10.

filter length of 10. A major change observed is the shift of the spectral peaks with different sample lengths. Previous studies of MEM have also shown shifts in spectral peaks with variations in the number of data samples (Chen and Stegen, 1974). The quality of the spectrum generally degrades with decreasing sample length. This is in accord with Chen and Stegen's (1974) observation that for very short data lengths the poor resolution and the instability (spurious detail) are a trade-off.

Depth estimates of the same profile used in the experiment of Figure 3 were obtained using a 41-point gate. The sequence of points is advanced by one point after calculation of each estimate till the entire data is used. The results are shown in Figure 5. The estimates generally converge on the true value with a maximum error of 15%. Since each estimate is an average for the entire sample length, variations in the magnetic basement with wavelengths of the order of the gate-length or smaller cannot be detected. Also, since the magnetic effect at each location is the superposition of effects from all locations, we are faced with an averaging effect inherent in analysis of magnetic data. It would be ideal if the magnetic effect due to each locality could be isolated from effects of other locations. This is physically impossible and mathematically unrealizable. Alternatively, we can employ an adaptive filter which maximizes the magnetic effect due to each location for the purpose of depth-determination. We

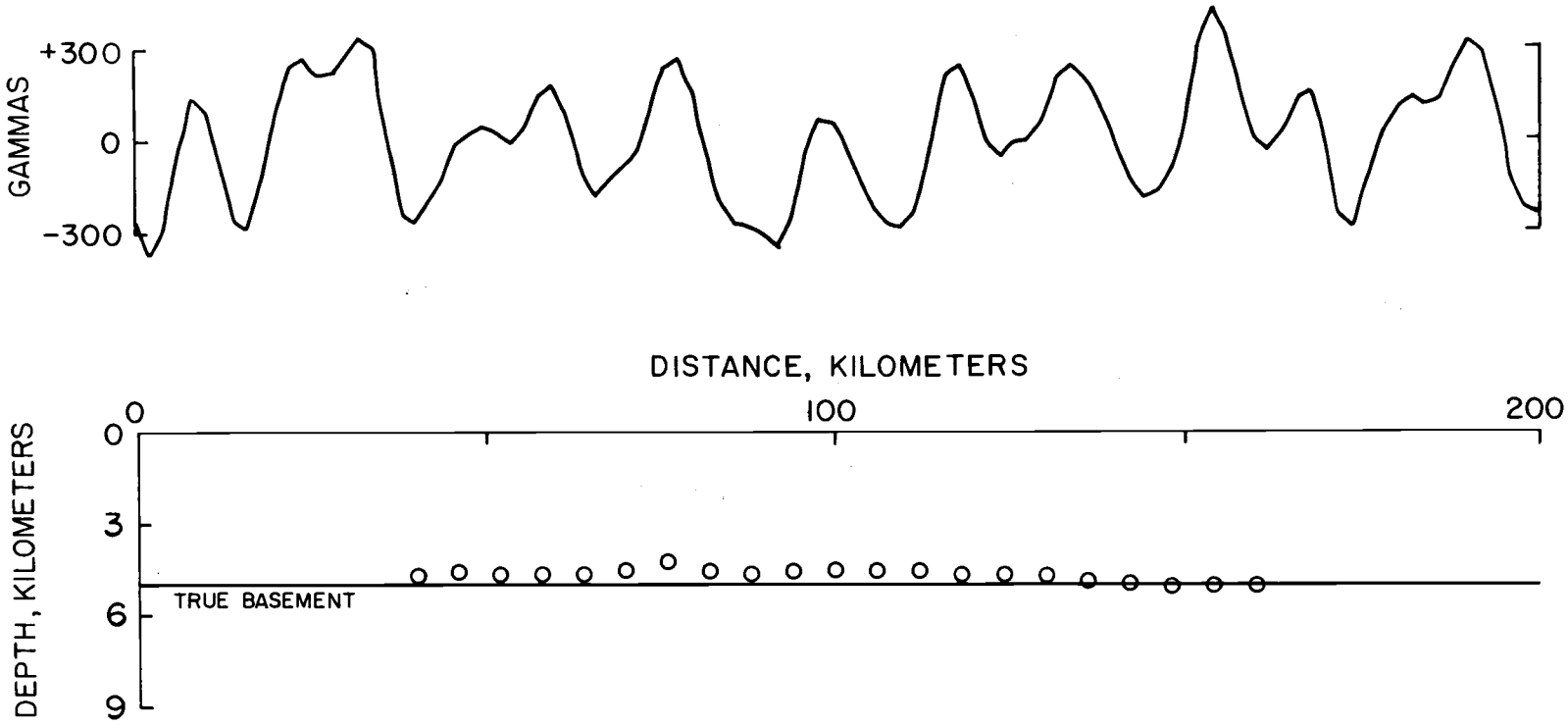

Figure 5. Test of the method on the magnetic profile of Figure 3. The profile (shown above) contains 101 data points with a uniform sampling increment of 2 km. The depth estimates (circles) were obtained using a 41-point gate. NPEF = 10.

have tried this and find that such filtering produces transients in the results, yielding unacceptable depth estimates. The cause of the breakdown is not known. It could be due to the type of the filter used, computational procedure employed, or both. Experiments with different filters might be desirable to enhance the applicability of such a technique.

A perfectly uncorrelated magnetic distribution is only an ideal model which is not often observed. To more accurately model the magnetization of oceanic crust, we tested the method on data generated from hypothetical crust with 11 magnetic reversals and with 50% white noise added. The location of the magnetic reversals were randomly chosen to conform with the random distribution of the reversals of the geomagnetic field (Cox, 1968, 1969). Depth estimates for such a model are shown in Figure 6. The estimates are consistently deeper than the true depth but the systematic deviation lies within 25% of the true depth. This is due to the fact that if the magnetization is correlated, its power spectrum is no longer constant, and this increase in the value of the power spectrum would result in the steepening of the spectral curves. This in turn would yield deeper estimates. Phillips (1975) also indicates that the autocorrelation analysis would yield deeper estimates if the magnetic distribution is correlated.

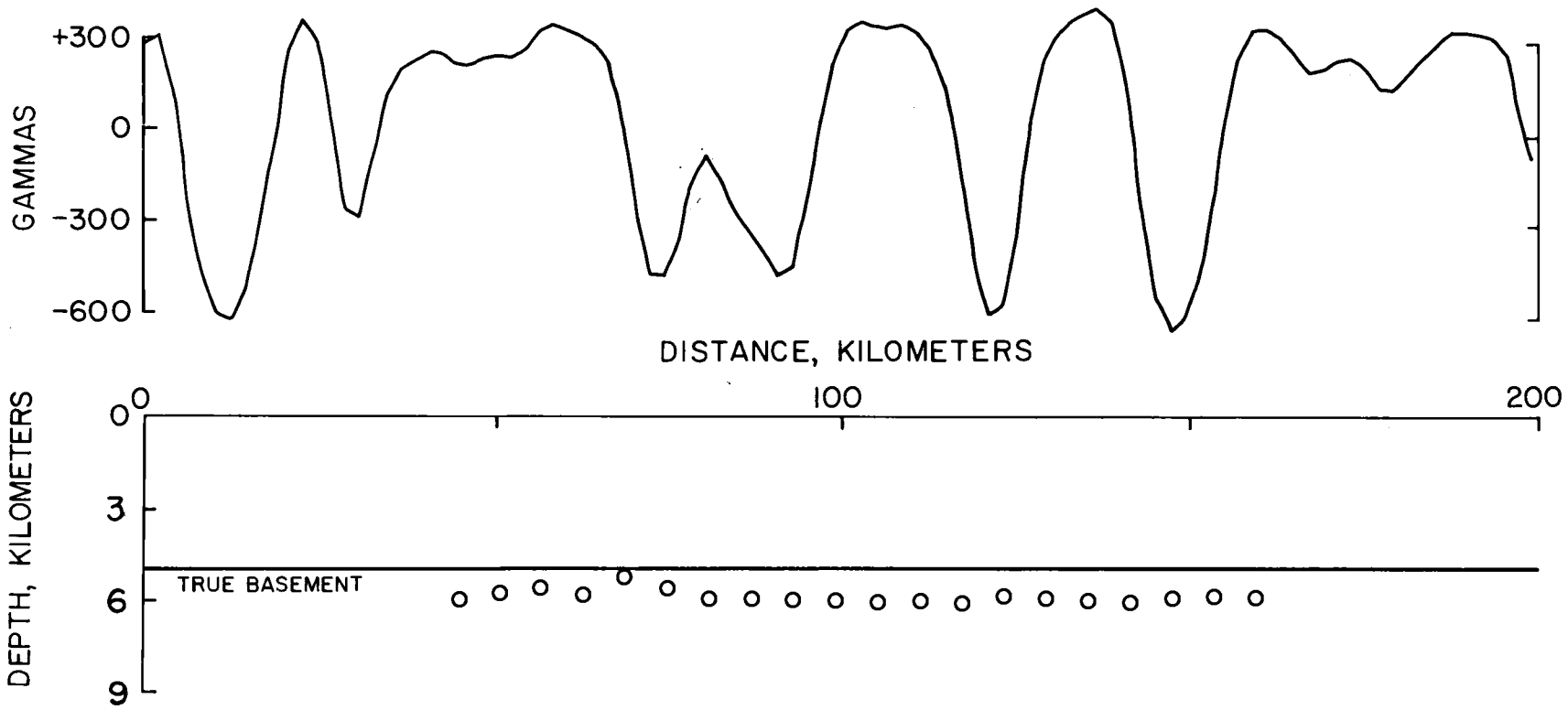

Figure 6. Depth estimates for a model containing reversed-polarity magnetization superimposed with 50% white noise. The profile (shown above) consists of 101 data points obtained at a uniform sampling increment of 2 km. Gate-length = 41, NPEF = 10.

The final test of the method was made on a step model with random intensity magnetization. The model is a one-kilometer thick, horizontal layer with a two-kilometer vertical offset in the middle of the layer. The magnetic profile for this model contains 200 data points obtained at a uniform sampling increment of 1 km. The intent of such a test was to examine the response of the method to depth changes in the magnetic basement. Depth estimates for such a model are shown in Figure 7. Figure 7a are depth estimates determined with the entire spectrum whereas 7b is estimates made by excluding the highest wavenumbers. In the former case, the estimates for the deeper basement are consistently shallower than the actual depth, whereas estimates for the shallow basement agree quite reasonably with the true value. Note that the estimates near the offset in the basement become unstable, and that these spurious results occur on the side of the deeper basement. This is believed to be due to the non-stationarity effect caused by the abrupt offset in the basement. Since the magnetic effect of shallow sources of equal intensity prevail over that of deeper basement, this effect is observed over the deeper sources. In the latter case, the estimates for the deeper basement improved and the estimates for the shallow basement still converge reasonably well. Empirical tests, such as described in Figure 7, indicate that abrupt offsets at depths of 3 km can be resolved within about 20 km.

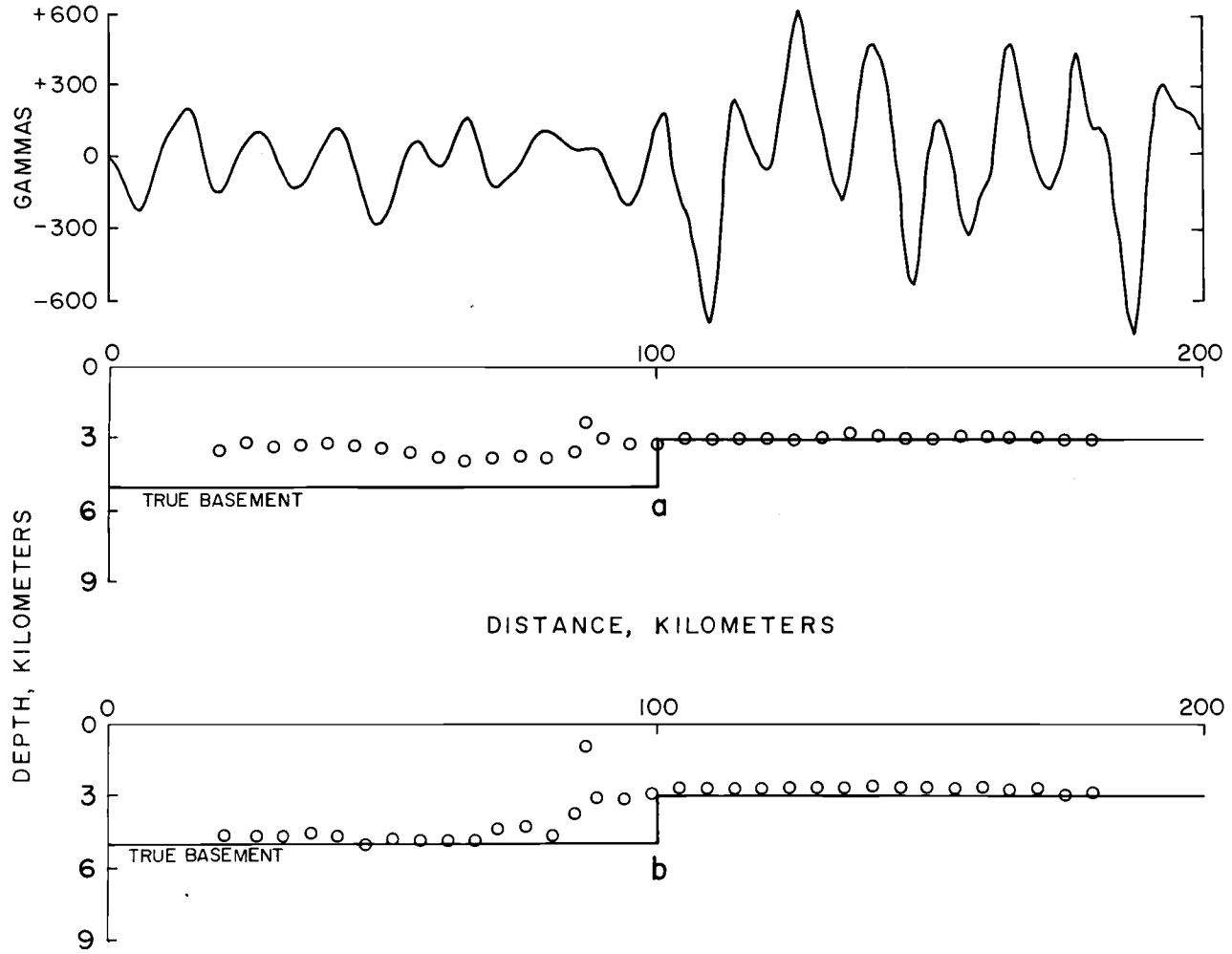

Figure 7. Depth estimates for a step model with random intensity magnetization. The profile (shown above) contains 200 data points with a uniform sampling increment of 1 km. The estimates at the bottom were obtained after excluding the portion of the spectral estimates at wavenumbers larger than half of the Nyquist. Gate-length = 41, NPEF = 10.

The above discussions indicate that the present depth determination technique can be applied to empirical data with reasonable results. In regions where some correlation in the magnetic distribution is suspected, interpretation of the results should be made taking into account the fact that the estimates would be generally deeper than the true depth. Unstable results may occur near regions of abrupt offset in the basement. If the magnetic basement is extremely irregular no valid results may be obtained other than an average value for the entire basement under investigation. However, if the undulations in the basement have wavelengths of the same order (or larger) as the window, the method might detect such undulations with reasonable accuracies. It might seem appropriate to express the limitations of the technique quantitatively. However, as regional conditions vary greatly with locality, such an attempt would not be fruitful. Instead, other geological and geophysical considerations should serve as constraints in interpretation of the results of such a method.

APPLICATION TO MARINE ANOMALIES OVER THE PERU-CHILE TRENCH

Magnetic anomalies from the northern Chile Trench were analyzed using the present depth estimation method and the autocorrelation technique of Phillips (1975). The data used in this study were collected by the research vessels YAQUINA of Oregon State University (OSU), the OCEANOGRAPHER of the National Oceanic and Atmospheric Administration (NOAA) and the MELVILLE of Scripps Institution of Oceanography. The collection of this data was sponsored by the National Science Foundation as a part of the International Decade of Ocean Exploration Nazca Plate Project involving joint investigations by the Hawaii Institute of Geophysics, NOAA, and OSU. The profiles analyzed in this paper traverse the area between latitudes 23°S and 31°S, and longitudes 70°W and 75°W (Figure 8).

Geologically, the Chile Trench is a part of the longer Peru-Chile Trench which is a narrow tectonic feature closely paralleling the entire west coast of South America. Island-arc-like tectonic features, volcanism, and orogeny associated with the trench have identified it as a major zone of convergence between an oceanic and a continental lithospheric plate. Studies of earthquake mechanisms (Isacks, 1970; Stauder, 1973, 1975) indicate that between the equator and the Chile Rise the oceanic Nazca plate underthrusts the South American continent. The rate of convergence of the Nazca plate

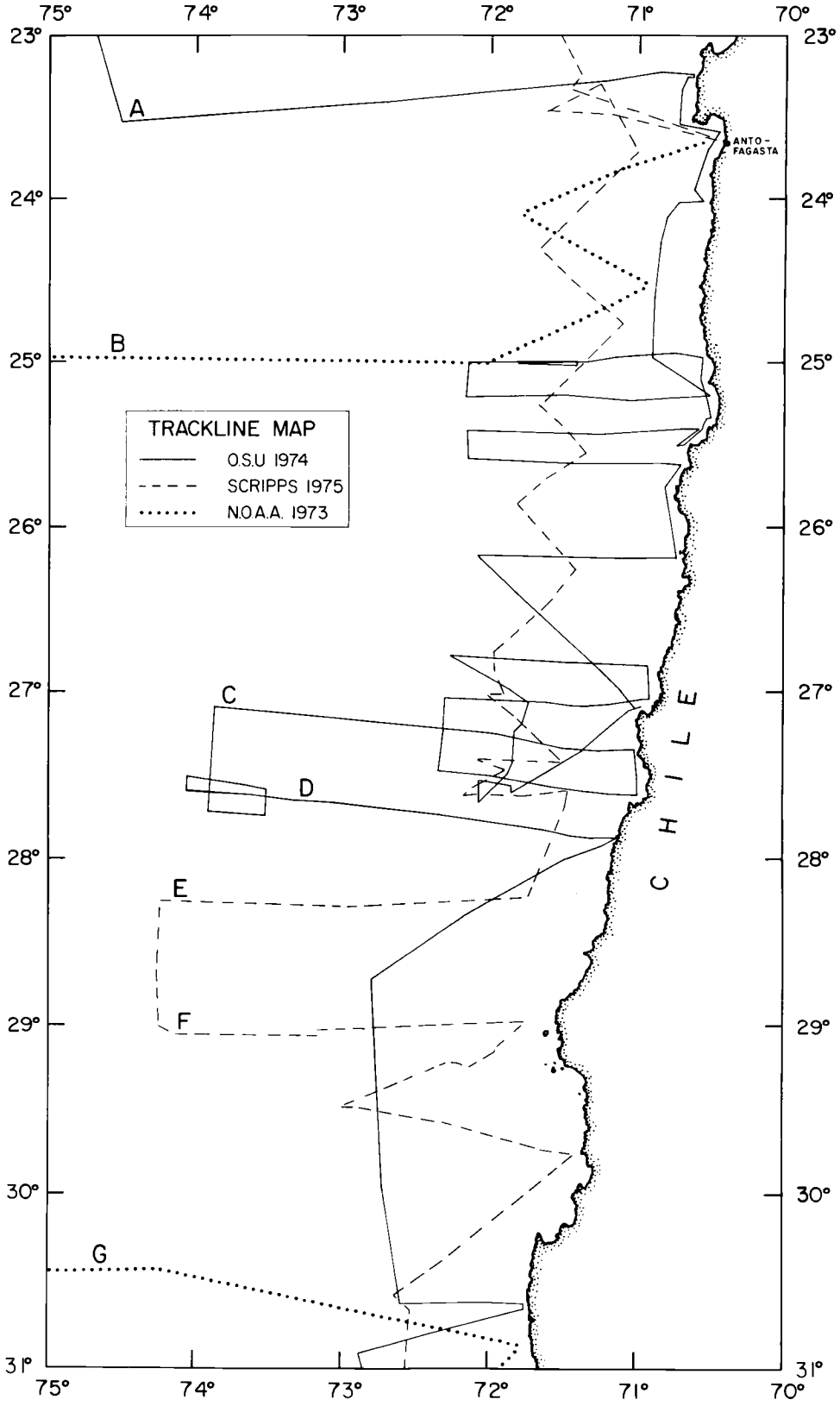

Figure 8. Trackline map. Lines labelled A through G are those used in Figure 10.

relative to South America is estimated to be 10 cm/yr (Minster and others, 1974).

Geological and geophysical investigations of the Peru-Chile trench prior to the concept of plate tectonics provided a very general picture of this margin (see Hayes (1966) for example). Recent concentrated field studies as a part of the Nazca Plate Project, however, are providing a detailed description of the Nazca plate-South American plate interface. Investigations now completed indicate a more complex tectonic process for the subduction zone than previously suspected (Kulm and others, 1973; Prince and others, 1974; Prince and Kulm, 1975; Hussong and others, 1975a, b; Whitsett, 1975). The analysis undertaken here is an attempt to investigate the nature of the subduction process as it affects the magnetic properties of the ocanic crust.

Magnetic Anomalies

The magnetic patterns in the eastern Pacific Ocean basin have a sea-floor spreading origin (Vine and Matthews, 1963) and date the crust adjacent to the trench between latitudes 23°S and 31°S as approximately 50 MY old (Herron, 1972; Hayes, 1974). In Figure 9, the anomalies are shown plotted along the trackline. Although the anomalies are most complex in this area, correlation has been attempted as shown by the dashed lines. Herron (1972) suggested that these anomalies outline a fossil ridge which apparently trended

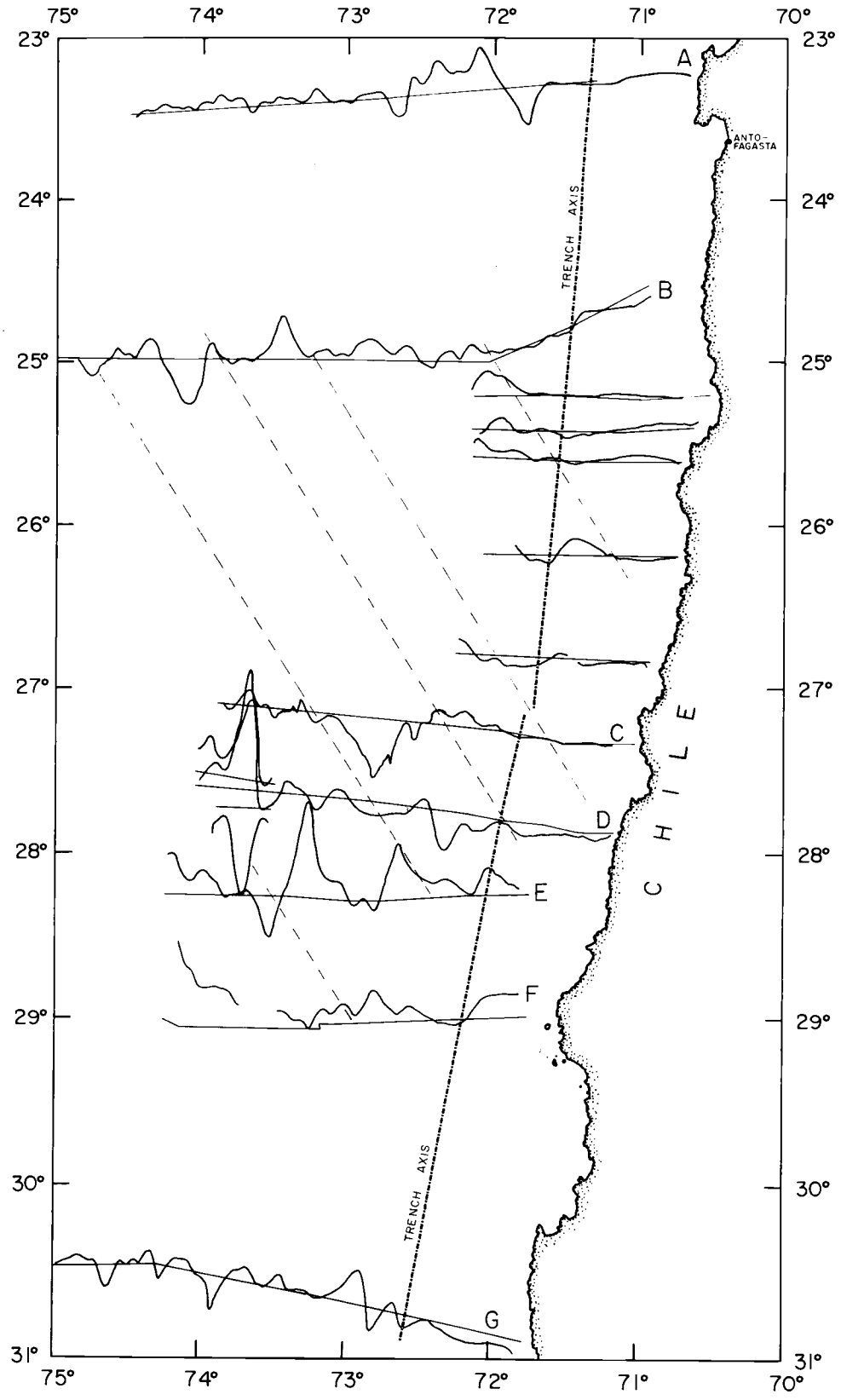

Figure 9. Selected profiles of total intensity magnetic anomaly of the northern Chile trench. The dashed lines are the proposed trend of the anomalies.

N 10°W when it ceased spreading. Our observation of the magnetic anomalies adjacent to the trench indicate that the older magnetic anomalies trend even further to the west, approximately N 30°W (Figure 9).

The amplitudes of these sea-floor spreading magnetic lineations become rapidly attenuated upon crossing the trench axis, as also observed by Hayes (1974). Studies for other areas have indicated that this attenuation in amplitude cannot be explained solely by the increase in depth of the descending oceanic crust beneath the continental margin (Hayes, 1974).

Depth to magnetic basement was determined from seven of the longest profiles, labeled A through G in Figure 8. The results, using both the new method and the method of Phillips (1975) are shown in Figure 10. The value of the log-power spectrum at zero wavenumber (i.e., D C bias) and those at larger wavenumber that fall below 1% of the spectral peaks were excluded from the calculations. The thickness assigned to the oceanic magnetic layer was 1 km based on seismic refraction studies of the oceanic Nazca plate (Hussong and others, 1975a). The autocorrelation analysis technique of Phillips (1975), on the other hand, assumes infinite thickness.

The results from both methods generally indicate that, seaward of the trench axis, the magnetic basement lies near the observed topography (Figure 10). This agrees with seismic refraction studies

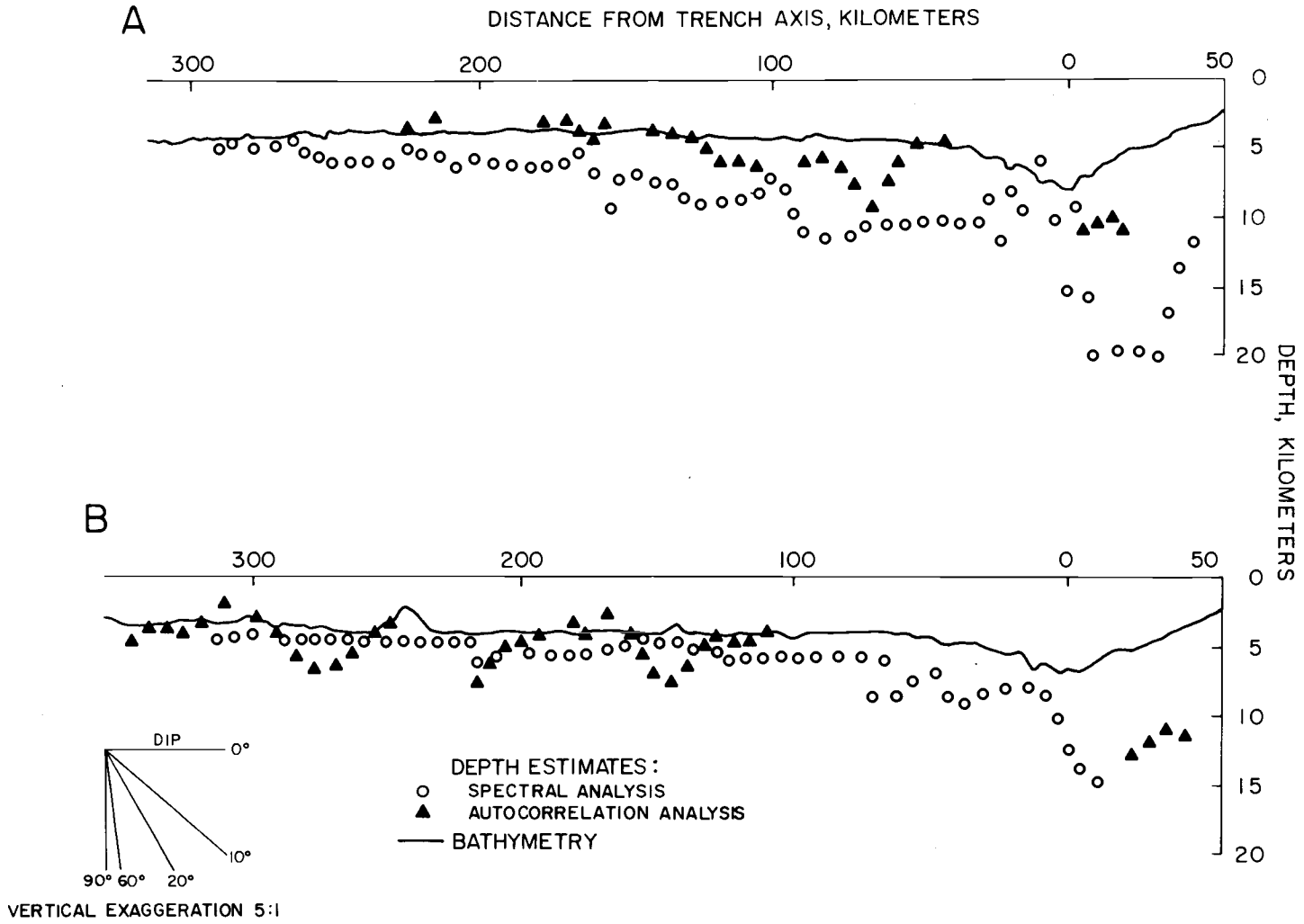

Figure 10. Depth estimates of the profiles in Figure 9 obtained using the new method and the autocorrelation analysis technique of Phillips (1975). The gate-length for the estimates obtained by spectral analysis is 41, NPEF = 10, and the sampling intervals are within the range of 1 to 2 km.

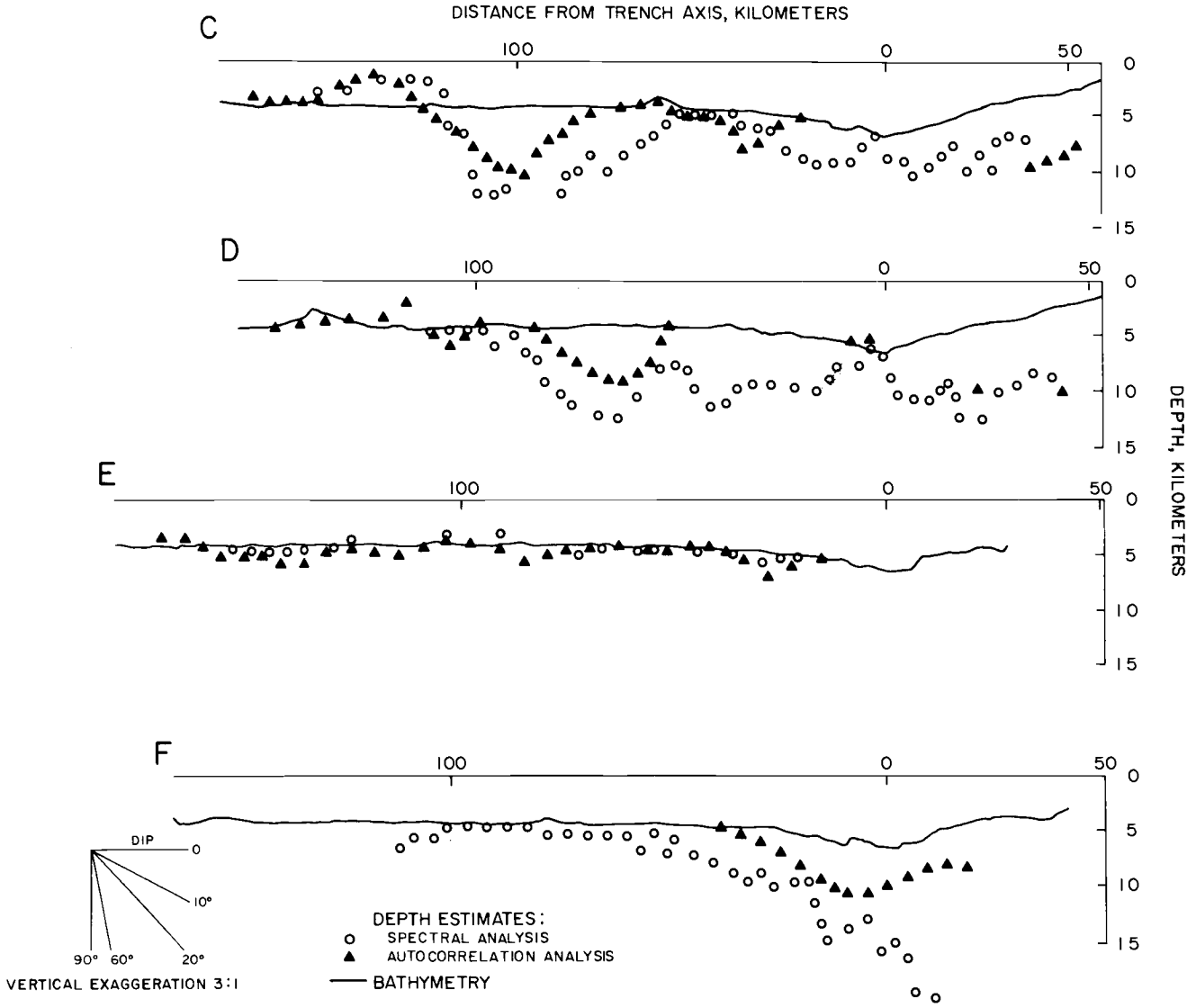

Figure 10. Continued.

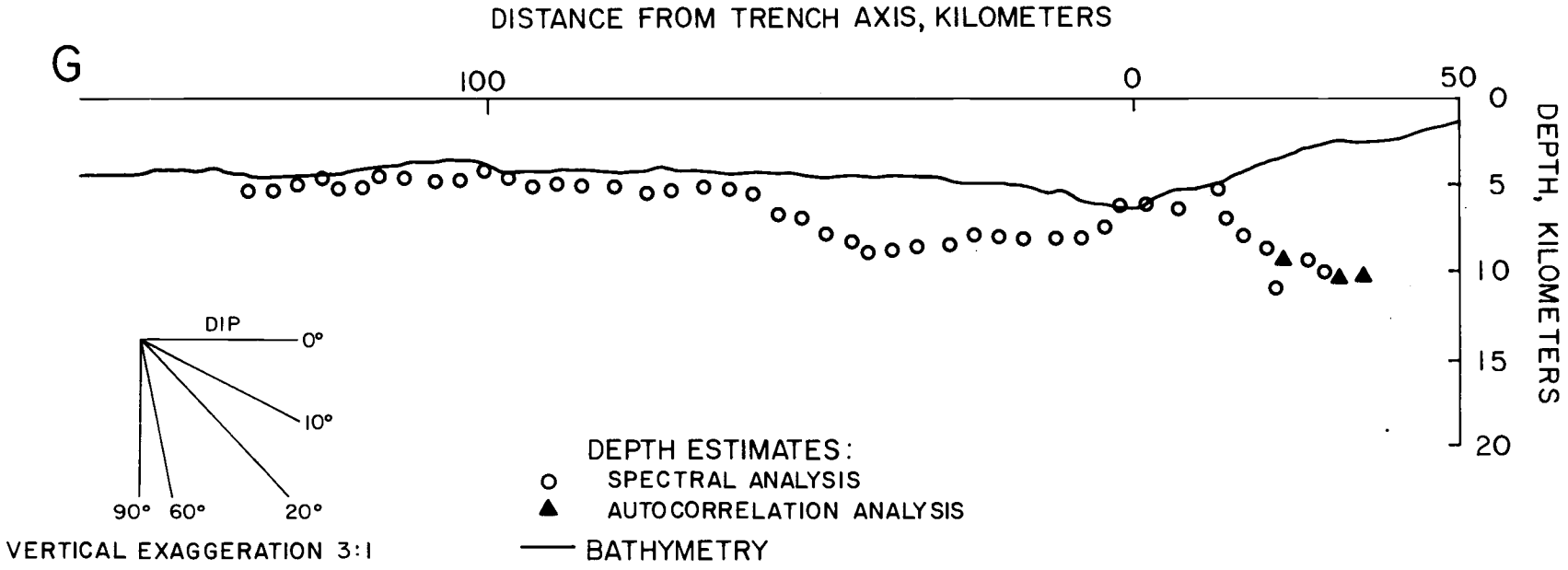

Figure 10. Continued.

on the Nazca plate which suggest a very thin (less than 200 meters) sedimentary layer lies atop the magnetic layer (Hussong and others, 1975a). As the plate approaches the subduction zone, the magnetic basement deepens. Seismic reflection studies of this region, however, do not indicate the thickening of layer 1 (i.e., the sedimentary layer) approaching the continent, so that the basaltic surface of layer 2 (i.e., the magnetic layer) is not deepening (Schweller, 1976). Apparently the spectral depth estimates near the seaward trench-slope are deeper than the actual basement. This would result if the actual thickness of the magnetic layer is larger than the assumed value of 1 km. The increase in thickness required to raise the estimates to their expected level is, however, larger than physically possible because of temperature constraints. Alternatively, the shallow basement that Schweller (1976) has described near the trench slope may have lost part of its magnetization because of tectonic disturbances so that the more important magnetic sources are deeper. Since a thickening layer cannot be distinguished from a deepening source, we cannot decide on the best answer. In fact, the observed deepening may be a combination of both effects.

The thickening of the oceanic crust would require the presence of horizontal compressional stresses. The presence of a compressional stress regime was suggested by Mendiguren (1971) who determined a dip-slip model with an east-west-oriented horizontal

pressure axis for a shallow shock in the middle of the Nazca plate. Studies of other mid-plate earthquakes recorded elsewhere in the world indicate similar results (Sykes and Sbar, 1973). Also, recent studies of the Nazca plate show compressional faulting of the oceanic crust prior to the subduction in the Peru-Chile Trench (Hussong and others, 1975b) and wide-angle seismic reflection profiling of the Peru Trench suggest the thickening of the oceanic crust as it plunges beneath the continental slope (Goebel, 1974). Therefore, general thickening of the oceanic layer is a definite possibility.

The compressional stress regime may also be the cause of the demagnetization of the magnetic material because of disruption of the basaltic layer. This would be true despite indications that the seaward slope of the trench is under tension (Schweller, 1976). Tensional stresses are also seen in other areas but are confined only to small regions along the line of flexure and only to the uppermost skin of the bending lithosphere (Hussong and others, 1975b). Attenuation of the magnetic anomalies in other trenches are attributed to the demagnetization of the crust by tectonic processes (Grow and Mudie, 1973).

Another way to demagnetize downgoing magnetic material is by heating of the descending slab. This idea is rejected on the basis of thermal studies which indicate that the downgoing slab maintains its temperature and rigidity to great depths (McKenzie, 1969: Minear and

Toksoz, 1970a, b; Toksoz and others, 1971). Heating due to friction would also be negligible at shallow depths (Turcotte and Schubert, 1973). Hence, demagnetization due to heating to temperatures above the Curie temperature of the magnetic material would be unlikely. Therefore, in regions where the increase in depth-to-source cannot alone explain the attenuation of the magnetic anomalies, tectonic deformation would most likely be the cause. Such attenuations are accentuated upon crossing the trench axis where the opposing plate motions cause the reversal of the stress types to compressional within the upper oceanic crust (Schweller, 1976).

The depth estimates for the regions underlying the continental slope (i.e., east of the trench axis) are generally scattered and less reliable since the amplitudes of the anomalies are lower. Where estimates are obtained, they are within the toe of the continental margin. Since the continental rocks in this area have very low magnetic susceptibilities (Mordojovich, 1974), it is believed that the magnetic effect observed over the continental slope is due to sources with an oceanic origin. This implies penetration and possible uplift of oceanic material into the continental slope. Such uplifts of oceanic material have been suggested for regions further north (Prince and Kulm, 1975; Hussong and others, 1975a). Also, geophysical investigations of the continental shelf off Western Guatemala suggest presence of high density block in the lower slope which may be a

melange of sediments and oceanic basement (Woodcock, 1975). This is further supported by the fact that there are no high wavenumber components in the observed magnetic anomalies to indicate the presence of shallow interbedded sediments within volcanics. Nevertheless, other geophysical considerations are required to determine if crustal rupture and uplift of this magnitude actually occur in this region.

Overall, the magnetic basement is observed to be a continuous feature with no major discontinuities except for the mid-plate irregularities observed in the profiles C, at approximately 100 km from the trench, and in profile D, at approximately 70 km from the trench. The apparent discontinuities in those profiles are located 75 km east of a structure which exhibits magnetic features typical of a seamount (Figure 9). The amplitudes of the magnetic anomalies observed over this feature are approximately twice as large as the average value for the magnetic pattern of the adjacent basin. This suggests that this feature is younger than the surrounding basin and may be the result of mid-plate volcanism. Such tectonism would cause the disruption of the oceanic basaltic layer upon their formation, but since those offsets are observed some distance from the proposed seamount, their relation to such tectonism is not certain. It is possible that the prevailing magnetic effect of the seamount causes a shift in the location of the apparent discontinuities. In that case, the actual

offsets, if any, would be much closer to this feature than indicated. An alternative explanation would be that there is a gap in the magnetization of the oceanic crust. But again this would require some type of mid-plate tectonism as it would be unlikely that the oceanic layer did not acquire remanent magnetization at the time of its formation.

SUMMARY AND CONCLUSIONS

In the past, spectral analysis of magnetic profiles has been restricted to areas of little topographic expression and, in general, has been used to look only at source parameters averaged over large regions. This restriction has been largely due to the poor response of the conventional power spectral estimators in the presence of non-stationary data. The proposed method of depth-to-basement calculation applies Burg's maximum entropy method to the estimation of power spectra. The advantage of this technique is to permit analysis of short segments of data in order to detect short wavelength changes in the spectral quality of data. Results indicate that abrupt offsets at a depth of 3 km can be resolved within a lateral distance of approximately 20 km.

The quality of the maximum entropy spectral estimates, however, generally degrades with decreasing data length. This results in a trade-off situation between high resolution and good spectral estimates. Particularly, when the theoretical power spectrum is not known, there is no means, a priori, of determining the optimum gate-length. For such cases, other geological and geophysical considerations should serve as constraints in the interpretation of the results. Comparison with depth estimates obtained using other techniques may also be used to determine the validity of the results of this method.

The application of the method to theoretical data and marine profiles from the Peru-Chile trench has yielded encouraging results. For the eastern margin of the Nazca plate, they generally indicate a continuous magnetic basement extending into the subduction zone. The basement is shallow seaward of the trench axis and deepens as the plate approaches the convergent margin. This apparent deepening is postulated to be due to the thickening and the deterioration of the magnetization of the oceanic crust caused by the compressional disruption of the basaltic layer. Landward of the trench axis, the depth estimates indicate possible uplift of the oceanic material into the lower slope of the continental margin.

The maximum entropy method provides substantial improvement in the resolution of statistical techniques for the analysis of magnetic data. Further quantitative analysis is required to enhance the applicability of such methods. Recent advances in spectral analysis based on the final prediction error statistic of Akaike (1969, 1970) may provide such a means.

BIBLIOGRAPHY

Akaike, H., 1969, Power spectrum estimation through auto-regressive model fitting, Ann. Inst. Stat. Math. (Tokyo), 21, 407-419.

Akaike, H., 1970, A fundamental relation between predictor identification and power spectrum estimation, Ann. Inst. Stat. Math. (Tokyo), 22, 219-233.

Bhattacharyya, B.K., 1966. Continuous spectrum of the total magnetic field anomaly due to a rectangular prismatic body, Geophysics, 31, 97-121.

Blackman, R.B. and J.W. Tukey, 1959, The measurement of power spectra, Dover Publications, Inc., New York.

Blakely, R.J. and A. Cox, 1972, Identification of short polarity events by transforming marine magnetic profiles to the pole, J. Geophys. Res., 77, 4339-4349.

Bott, M.H.P., 1967, Solution of the linear inverse problem in magnetic interpretation with application to oceanic magnetic anomalies, J.R. Astr. Soc., 13, 313-323.

Bracewell, R.N., 1965, The Fourier transform and its applications, McGraw-Hill Book Co., Inc., New York.

Burg, J.P., 1967, Maximum entropy spectral analysis, paper presented at the 37th meeting, Soc. Explor. Geophys., Oklahoma City, Okla.

Burg, J.P., 1968. A new analysis technique for time series data, paper presented at NATO Advanced Study Institute on Signal Processing, Enschede, Netherlands.

Burg, J.P., 1970, New concepts in power spectra estimation: paper presented at 40th Annual International SEG Meeting, New Orleans, Louisiana.

Chen, W.Y. and G.R. Stegen, 1974, Experiments with maximum entropy power spectra of sinusoids, J. Geophys. Res., 79, 3019-3022.

Claerbout, J.F., 1970, Waveforms analysis, unpublished manuscript.

Cooley, J.W. and J.W. Tukey, 1965, An algorithm for the machine calculations of complex Fourier series, Math. of Comp., 19, 297-301.

Cox, A., 1968, Lengths of geomagnetic polarity intervals, J. Geophys. Res., 73, 3247-3260.

Cox, A., 1969, Geomagnetic reversals, Science, 163, 237-245.

Denham, C.R., 1975, Spectral analysis of paleomagnetic time series, J. Geophys. Res., 80, 1897-1901.

Fryer, G.J., M.E. Odegard, and G.H. Sutton, 1975, Deconvolution and spectral estimation using final prediction error, Geophysics, 40, 411-425.

Goebel, V., 1974, Modeling of the Peru-Chile Trench from wide angel reflection profiles, M.S. thesis, Oregon State University, Corvallis, Oregon, 88 p.

Grow, J.A. and J.D. Mudie, 1973, Attenuation of Pacific magnetic anomalies in the Aleution Trench (abstracts) EOS Transactions, AGU, 54, 330.

Gudmundsson, G., 1966, Interpretation of one-dimensional magnetic anomalies by use of the Fourier transform, Geophys. J.R. Astra. Soc., 12, 87-97.

Hayes, D.E., 1966, A geophysical investigation of the Peru-Chile Trench, Marine Geology, 4, 309-351.

Hayes, D.E., 1974, Continental margin of western South America, In: C.A. Burk and C.L. Drake (eds.), The Geology of Continental Margins, Springer-Verlag, New York, 581-590.

Herron, E.M., 1972, Sea-floor spreading and the Cenozoic history of the east-central Pacific, Geol. Soc. America Bull., 83, 1671-1692.

Hussong, D. M., P. B. Edwards, S. H. Johnson, J. F. Campbell, and G. H. Sutton, 1975a, Crustal structure of the Peru-Chile Trench: 8°-12°S latitude, in G. H. Sutton, M. H. Manghnani, and R. Moberly (eds.), The Geophysics of the Pacific Ocean basin and its margin (Wollard colume), AGU Geophys. Mon. 19 (in press).

Hussong, D. M., M. E. Odegard, and L. K. Wipperman, 1975b, Compressional faulting of the oceanic crust prior to subduction in the Peru-Chile Trench, Geology, 3, 601-604.

Isacks, B., 1970, Focal mechanism of earthquakes in western South America (abstract), EOS Transactions, AGU, 51, 355.

Jones, R. H., 1965, A reappraisal of the periodogram in spectral analysis, Technometrics, 7, 531-542.

Jenkins, G. M. and D. G. Watts, 1968, Spectral analysis and its applications, Holden-Day, Inc., San Francisco, Calif.

Kanasewich, E. G., 1975, Time sequence analysis in geophysics, The University of Alberta Press, Edmonton, Alberta, Canada.

Kulm, L. D., K. F. Scheidegger, R. A. Prince, J. Dymond, T. C. Moore Jr., and D. M. Hussong, 1973, Tholeiitic basalt ridge in the Peru Trench, Geology, 1, 11-14.

Lacoss, R. T., 1971, Data adaptive spectral analysis methods, Geophysics, 36, 661-675.

Lee, Y. W., 1960, Statistical theory of communication, John Wiley and Sons, Inc., New York.

McKenzie, D. P., 1969, Speculations on the consequences and causes of plate motions, Geophys, J. R. Astr. Soc., 18, 1-32.

Mendiguren, J. A., 1971, Focal mechanism of a shock in the middle of the Nazca plate, J. Geophys. Res., 76, 3861-3879.

Minear, J. W. and M, N. Toksoz, 1970a, Thermal regime of a downgoing slab and new global tectonics, J. Geophys. Res., 75, 1397-1419.

Minear, J.W. and M.N. Toksoz, 1970b, Thermal regime of a downgoing slab, Tectonophysics, 10, 367-390.

Minster, J.B., T.H. Jordon, P. Molnar, and E. Haines, 1974, Numerical modeling of instantaneous plate tectonics, Geophys. J.R. Astr. Soc., 36, 541-576.

Mordojovich, K.C., 1974, Geology of a part of the Pacific margin of Chile, In: C.A. Burk and C.L. Drake (eds.). The Geology of Continental Margins, Springer-Verlag, New York, 591-597.

Nabighian, M.N., 1972, The analytic signal of two-dimensional magnetic bodies with polygonal cross-section: its properties and use for automated anomaly interpretation, Geophysics, 37, 507-517.

Nabighian, M.N., 1974, Additional comments on the analytic signal of two-dimensional magnetic bodies with polygonal cross-section, Geophysics, 39, 85-92.

Parker, R.L. and S.P. Huestis, 1974, The inversion of magnetic anomalies in the presence of topography, J. Geophys. Res., 79, 1587-1593.

Phillips, J.D., 1975, Statistical analysis of magnetic profiles and geomagnetic reversal sequences, Ph.D. Dissertation, Stanford University, Stanford, Calif., 134 p.

Prince, R.A., J.M. Resig, L.D. Kulm, and T.C. Moore Jr., 1974, Significance of uplifted turbidite basins on the seaward wall of the Peru Trench, Geology, 2, 607-611.

Prince, R.A. and L.D. Kulm, 1975, Crustal rupture and the initiation of imbricate thrusting in the Peru Trench, Geol. Soc. America Bull., 86, 1639-1653.

Puranen, M., V. Marmo, and U. Hamalainen, 1968. On the geology, aeromagnetic anomalies and susceptibilities of Precambrian rocks in the Virrat region (Central Finland), Geoexploration, 6, 163-184.

Schweller, W.J., 1976, Chile Trench: extensional rupture of oceanic crust and the influence of tectonics on sediment distribution, M.S. thesis, Oregon State University, Corvallis, Oregon, 80 p.

Serson, P.H. and W.L.W. Hannaford, 1957, A statistical analysis of magnetic profiles, J. Geophys. Res., 62, 1-18.

Spector, A. and F.S. Grant, 1970, Statistical models for interpreting aeromagnetic data, Geophysics, 35, 293-302.

Stauder, W., 1973, Mechanisms and spatial distribution of Chilean earthquakes with relation to subduction of oceanic plate, J. Geophys. Res., 78, 5033-5061.

Stauder, W., 1975, Subduction of the Nazca plate under Peru as evidenced by focal mechanisms and by seismicity, J. Geophys. Res., 80, 1053-1064.

Sykes, L. and M. Sbar, 1973, Intra-plate earthquakes, contemporary stresses and the driving mechanism of plate tectonics; Pt. 2, Global evidence (abstract), EOS Transactions, AGU, 54, 455.

Talwani, M., C.C. Windisch, and M.G. Langseth, 1971, Reykjanes ridge crest: a detailed geophysical study, J, Geophys. Res., 76, 473-517.

Toksoz, M.N., J.W. Minear, and B.R. Julian, 1971, Temperature field and geophysical effects of a downgoing slab, J. Geophys. Res., 76, 1113-1138.

Treitel, S., W.G. Clement, and R.K. Kaul, 1971, The spectral determination of depths to buried magnetic basement rocks, Geophys. J.R. Astr. Soc., 24, 415-428.

Turcotte, D.L. and G. Schubert, 1973, Frictional heating of the descending lithosphere, J. Geophys. Res., 78, 5876-5886.

Ulrych, T.J., 1972, Maximum entropy power spectrum of truncated sinusoids, J. Geophys. Res., 77, 1396-1400.

Ulrych, T.J., D.E. Smylie, O.G. Jensen, and G.K.C. Clarke, 1973, Predictive filtering and smoothing of short records by using maximum entropy, J. Geophys. Res., 78, 4959-4964.

Ulrych, T.J. and T.N. Bishop, 1975, Maximum entropy spectral analysis and autoregressive decomposition, Rev. Geophys. Space Phys., 13, 183-200.

Vine, F. J. and D. H. Matthews, 1963, Magnetic anomalies over ocean ridges, Nature, 199, 947-949.

Whitsett, R. M., 1975, Gravity measurements and their structural implications for the continental margin of southern Peru, PhD thesis, Oregon State University, Corvallis, Oregon, 82 p.

Wiley, C. R. Jr., 1966, Advanced engineering mathematics, McGraw-Hill Book Co., Inc., New York.

Woodcock, S. F., 1975, Crustal structure of the Tehuntepec ridge and adjacent continental margins of southwestern Mexico and western Guatemala, M. S. thesis, Oregon State University, Corvallis, Oregon, 52 p.

APPENDICES

APPENDIX I

Uncorrelated Distribution

For any magnetized body, the magnetization can be approximated by dividing the body into a large number of cells each having a lumped magnetization vector $\vec{m}_i$ in the i^{th} cell. We shall assume that $\vec{m}_i$'s are unidirectional but of random intensity such that

$$\begin{aligned} E\{m_i\} &= m_o \\ E\{(m_i - m_o)^2\} &= \sigma^2 \end{aligned} \qquad \text{for all i's} \qquad \text{(A.I.1)}$$

where E indicates the expectation value, m_0 is the mean, and σ^2 is the variance. The $\vec{m}_i$'s are uncorrelated if

$$E\{(m_i - m_o)(m_j - m_o)\} = \delta_{ij}\sigma^2 \qquad \text{(A.I.2)}$$

where δ_{ij} is the Kronecker delta function

$$\delta_{ij} = \begin{cases} 0 & i \neq j \\ 1 & i = j \,. \end{cases} \qquad \text{(A.I.3)}$$

APPENDIX II

As stated earlier, Equation 17 has more linear equations than unknowns. In such cases it is usually impossible to find a set of solutions which satisfy all of the equations. One must resort to methods which yield solutions which approximately satisfy all the equations (Claerbout, Waveform Analysis, unpublished manuscript, 1970). Let $a = (1/2) \ln A$, and $c_i = (1/2) \ln P_i - \ln(1-e^{-tk_i})$, $i = 0, \ldots, M$. Then the matrix representation of Equation 17 is

$$\begin{bmatrix} 1 & -k_0 \\ \vdots & \vdots \\ 1 & -k_M \end{bmatrix} \begin{bmatrix} a \\ z \end{bmatrix} = \begin{bmatrix} c_0 \\ \vdots \\ c_M \end{bmatrix} \qquad \text{(A.II.1)}$$

where a and z are the unknowns. Usually there will be no set of (a, z) which exactly satisfies (A.II.1). Let us define an error vector e_i by

$$\begin{bmatrix} 1 & -k_0 \\ \vdots & \vdots \\ 1 & -k_M \end{bmatrix} \begin{bmatrix} a \\ z \end{bmatrix} - \begin{bmatrix} c_0 \\ \vdots \\ c_M \end{bmatrix} = \begin{bmatrix} e_0 \\ \vdots \\ e_M \end{bmatrix} \qquad \text{(A.II.2)}$$

An equivalent representation of (A.II.2) is

$$\begin{bmatrix} -c_0 & 1 & -k_0 \\ \vdots & \vdots & \vdots \\ -c_M & 1 & -k_M \end{bmatrix} \begin{bmatrix} 1 \\ a \\ z \end{bmatrix} = \begin{bmatrix} e_0 \\ \vdots \\ e_M \end{bmatrix} \qquad \text{(A.II.3)}$$

If B, X, and e represent matrices containing the coefficients, unknowns, and the errors, respectively, (A.II.3) can be abbreviated by

$$BX = e \qquad \text{(A.II.4)}$$

The matrix X which makes the error vector as short as possible is our desired solution. The length of the error vector is

$$E = e^T e = e_0^2 + e_1^2 + \ldots + e_M^2 = \sum_{i=0}^{M} e_i^2 \qquad \text{(A.II.5)}$$

where e^T is the transpose of e (see Wiley, 1966, p. 415). Using (A.II.4), the error E can be expressed by

$$E = e^T e = (BX)^T (BX) = X^T (B^T B) X \qquad \text{(A.II.6)}$$

where

$$B^T B = \begin{bmatrix} -c_0 & \cdots & -c_M \\ 1 & \cdots & 1 \\ -k_0 & \cdots & -k_M \end{bmatrix} \begin{bmatrix} -c_0 & 1 & -k_0 \\ \vdots & \vdots & \vdots \\ -c_M & 1 & -k_M \end{bmatrix} =$$

$$= \begin{bmatrix} \sum_{i=0}^{M} c_i^2 & \sum_{i=0}^{M} c_i & \sum_{i=0}^{M} k_i c_i \\ \sum_{i=0}^{M} -c_i & \sum_{i=0}^{M} 1 & \sum_{i=0}^{M} -k_i \\ \sum_{i=0}^{M} k_i c_i & \sum_{i=0}^{M} -k_i & \sum_{i=0}^{M} k_i^2 \end{bmatrix}$$

$$= \begin{bmatrix} r_{11} & r_{12} & r_{13} \\ r_{21} & r_{22} & r_{23} \\ r_{31} & r_{32} & r_{33} \end{bmatrix}$$

$$= R \qquad \text{(A.II.7)}$$

Note that R is symmetric, i.e., $r_{ij} = r_{ji}$. Therefore, using (A.II.6) a different representation for E would be

$$E = [1 \quad a \quad z][R]\begin{bmatrix} 1 \\ a \\ z \end{bmatrix} \qquad \text{(A.II.8)}$$

To find the X with minimum E, we require $(\partial E/\partial a) = 0$, and $(\partial E/\partial z) = 0$, i.e.,

$$0 = \partial E/\partial a = [0 \quad 1 \quad 0][R]\begin{bmatrix} 1 \\ a \\ z \end{bmatrix} + [1 \quad a \quad z][R]\begin{bmatrix} 0 \\ 1 \\ 0 \end{bmatrix}$$

$$0 = \partial E/\partial z = [0 \quad 0 \quad 1][R]\begin{bmatrix} 1 \\ a \\ z \end{bmatrix} + [1 \quad a \quad z][R]\begin{bmatrix} 0 \\ 0 \\ 1 \end{bmatrix} \qquad \text{(A.II.9)}$$

Since R is symmetric, both terms on the right of each equation in (A.II.9) are equal. Hence, we can re-write (A.II.9) by

$$0 = 2[0 \quad 1 \quad 0][R]\begin{bmatrix} 1 \\ a \\ z \end{bmatrix}$$

$$0 = 2[0 \quad 0 \quad 1][R]\begin{bmatrix} 1 \\ a \\ z \end{bmatrix} \qquad \text{(A.II.10)}$$

Combining the two expressions in (A.II.10) and expressing R in terms of its components, we obtain

$$\begin{bmatrix} r_{21} & r_{22} & r_{23} \\ r_{31} & r_{32} & r_{33} \end{bmatrix}\begin{bmatrix} 1 \\ a \\ z \end{bmatrix} = \begin{bmatrix} 0 \\ 0 \\ 0 \end{bmatrix} \qquad \text{(A.II.11)}$$

or,

$$\begin{bmatrix} r_{22} & r_{23} \\ r_{32} & r_{33} \end{bmatrix}\begin{bmatrix} a \\ z \end{bmatrix} = \begin{bmatrix} -r_{21} \\ -r_{31} \end{bmatrix} \qquad \text{(A.II.12)}$$

which is a simple problem of two equations and two unknowns. The final expression for z is thus

$$z = \frac{\sum_{i=0}^{M} c_i \sum_{i=0}^{M} k_i - M \sum_{i=0}^{M} k_i c_i}{M \sum_{i=0}^{M} k_i^2 - \left(\sum_{i=0}^{M} k_i \right)^2} \qquad \text{(A.II.13)}$$

APPENDIX III

Program MAGDEPTH

MAGDEPTH is a FORTRAN IV program which uses maximum entropy spectral analysis to estimate depth to magnetic basement from evenly sampled magnetic profiles. The average value and the regional trend have to be removed from the data before processing by this program.

Inputs to the program are:

LABEL: output identification.

ND: the number of data points in the profile.

DX: the sample interval.

NX: the gate-length. The choice of NX is critical as it determines the resolution desired and the quality of the results. A starting value may be half the profile length (i.e., ND/2), but a minimum of 30 should be imposed as spurious estimates might result if a smaller length is employed. If only an average value is desired, NX should be set equal to ND.

NPEF: the number of terms in the prediction error filter. A reasonable range for NPEF is between 10 and 15.

DT: the assumed thickness of the model. The choice of DT is not critical as the results vary little for large changes in DT.

NFIRST: the first value of the Ln-power spectrum to be used in the calculation.

PERCENT: the high frequency spectral cutoff. The value of PERCENT is determined by the fraction of the spectral peak excluded from the calculation. e.g., 1% = .01.

The program also requires the following control statements:

EQUIP, 1 = input filename (i.e., magnetic data)

EQUIP, 2 = FILE

SAVE, 2 = output filename

EQUIP, 17 = LP

LABEL, 17/ your name

The formats in which the magnetic profile is to be read from and the output is to be written are (5(8X, F8.0)) and (10F7.2), respectively. They can, however, be modified if desired.

At the output stage, the depth estimates are printed and stored. An example of input/output procedure and the program are listed below.

```
#EQUIP,1=*MOD1
#EQUIP,2=FILE
#SAVE,2=TESTFILE
#EQUIP,17=LP
#LABEL,17/HASSANZADEH
#FORTRAN,I=MAGDEPTH,R
 NO ERRORS FOR MAGDEPTH
 NO ERRORS FOR MEPS
 NO ERRORS FOR NORBRT
 NO ERRORS FOR BURG
 NO ERRORS FOR LEVIN
 NO ERRORS FOR DEPTH
RUN

ENTER LABEL, FORMAT(10A8)
 DEPTH ESTIMATES FOR MODEL 1
ENTER INPUT PARAMETERS,(I5,F10.5,2I5,F10.5,I5,F10.5)
   51   2.        41    9    1.        5    .01



END OF FORTRAN EXECUTION
```

DEPTH ESTIMATES FOR MODEL 1

STATION	LOCATION	ANOMALY	DEPTH
1	0	-260	
2	2.000	-374	
3	4.000	-277	
4	6.000	-21	
5	8.000	140	
6	10.000	98	
7	12.000	-70	
8	14.000	-263	
9	16.000	-278	
10	18.000	-109	
11	20.000	95	
12	22.000	239	
13	24.000	270	
14	26.000	211	
15	28.000	216	
16	30.000	266	
17	32.000	335	
18	34.000	304	
19	36.000	38	
20	38.000	-241	
21	40.000	-265	5.70
22	42.000	-203	5.70
23	44.000	-132	5.56
24	46.000	-17	5.81
25	48.000	16	5.90
26	50.000	47	5.84
27	52.000	26	5.87
28	54.000	-10	5.79
29	56.000	45	5.74
30	58.000	147	5.63
31	60.000	180	5.49
32	62.000	81	
33	64.000	-83	
34	66.000	-182	
35	68.000	-141	
36	70.000	-89	
37	72.000	-41	
38	74.000	110	
39	76.000	238	
40	78.000	265	
41	80.000	162	
42	82.000	-44	
43	84.000	-209	
44	86.000	-270	
45	88.000	-274	
46	90.000	-299	
47	92.000	-343	
48	94.000	-253	
49	96.000	-43	
50	98.000	65	
51	100.000	59	

```
      PROGRAM MAGDEPTH
      REAL X(1000),DT,LABEL(10),XX(1000),XA(1000),D(1000),S(1000)
      WRITE(61,100)
      READ(60,101)LABEL
      WRITE(17,101)LABEL
      WRITE(61,102)
      READ(60,103)ND,DX,NX,NPEF,DT,NFIRST,PERCENT
      WRITE(61,103)ND,DX,NX,NPEF,DT,NFIRST,PERCENT
      READ(1,104)(XA(I),I=1,ND)
      PERCENT=-ALOG(PERCENT)
      PI=3.1415927
      DK=PI/(DX*FLOAT(NX-1))
      IP=NX/2+1
      NN=ND-NX/2
      NE=ND-NX+1
      IER=0
      K=0
1     DO 10 I=1,NX
      J=I+K
10    X(I)=XA(J)
      CALL MEPS(X,NX,S,NPEF,IER)
      K=K+1
      CALL DEPTH(S,DK,DT,D,IP,NFIRST,PERCENT,NX)
      IF(K.GE.NE)GO TO 99
      GO TO 1
99    CONTINUE
      DO 88 I=1,ND
88    XX(I)=FLOAT(I-1)*DX
      IN1=NX/2
      IN2=NN+1
      IN3=NX/2+1
      WRITE(17,105)
      WRITE(17,106)(I,XX(I),XA(I),I=1,IN1)
      WRITE(17,107)(I,XX(I),XA(I),D(I),I=IN3,NN)
      WRITE(17,106)(I,XX(I),XA(I),I=IN2,ND)
      WRITE(2,108)(D(I),I=IN3,NN)
100   FORMAT(X,≠ENTER LABEL, FORMAT(10A8)≠)
101   FORMAT(10A8)
102   FORMAT(X,≠ENTER INPUT PARAMETERS,(I5,F10.5,2I5,F10.5,I5,F10.5)≠)
103   FORMAT(I5,F10.5,2I5,F10.5,I5,F10.5)
104   FORMAT(5(8X,F8.0))
105   FORMAT(X,≠STATION≠,5X,≠LOCATION≠,5X,≠ANOMALY≠,5X,≠DEPTH≠,/)
106   FORMAT(3X,I3,5X,F8.3,5X,F8.0)
107   FORMAT(3X,I3,5X,F8.3,5X,F8.0,4X,F6.2)
108   FORMAT(10F7.2)
      STOP
      END
```

```
      SUBROUTINE MEPS(X,NX,S,NPEF,IEP)
      REAL X(1000),C(1000),EP(1000),EM(1000),A(1000),S(1000)
C
C.....................................................................
C
C     SUBROUTINE MEPS FINDS THE MAXIMUM ENTROPY POWER SPECTRUM
C  OF A REAL TIME SERIES.
C
C  INPUTS...
C     X  - THE TIME SERIES ARRAY.
C     NX - THE LENGTH OF THE TIME SERIES
C     NX - DESIRED LENGTH OF THE POWER SERIES.
C     NPEF - THE LENGTH OF THE PREDICTION ERROR FILTER.
C          NOTE THAT NPEF MUST BE LESS THAN OR EQUAL TO NX.
C
C  OUTPUTS...


C     S  - POWER SPECTRUM ARRAY WITH LENGTH NX.
C          NOTE THAT S(NX) IS THE POWER SPECTRUM AT THE
C          NYQUIST FREQUENPEFY AND S(1) IS THE POWER SPECTRUM
C          AT ZERO FREQUENPEFY.
C     IER- IF(NPEF.GT.NX)IER=1.  OTHERWISE, IER=0
C
C  WRITTEN BY RICK BLAKELY -- COMPLETED AUGUST 15, 1974
C  LIST MODIFICATIONS BELOW WITH DATES.
C
C.....................................................................
C
C  --  CHECK FOR ERROR
C
      IER=0
      IF(NPEF.LE.NX)GO TO 40
      IER=1
   40 CONTINUE

C
C  --  CALL BURG FOR REFLECTION COEFFICIENTS C
C
      CALL BURG(NX,X,NPEF,C,EP,EM)
C
C  --  CALL LEVIN FOR PREDICTION ERROR FILTER
C
      CALL LEVIN(C,NPEF,A)
C
C  --  CALL NORBRT FOR POWER SPECTRUM OF FILTER
C
      CALL NORBRT(A,NPEF,DX,S,NX)
C
C  --  FIND NORMALIZING POWER
C
      P=0.
      DO 20 I=1,NX
   20 P=P+X(I)**2
      P=P/FLOAT(NX)
      DO 30 I=2,NPEF
   30 P=P*(1.-C(I)**2)
C
C  --  INVERT SPECTRUM AND SCALE
C
      DO 10 I=1,NX
   10 S(I)=P/S(I)
      RETURN
      END
```

```
      SUBROUTINE NORSRT(X,NX,DX,S,NY)
      REAL X(1000),S(1000),A(1000)
C
C   AUTOCORRELATE THE INPUT
C
      DO 10 I=1,NX
   10 A(I)=0.
      DO 20 I=1,NX
      NN=NX-I+1
      DO 20 J=1,NN
      IPJM1=I+J-1
   20 A(J)=A(J)+X(I)*X(IPJM1)
C
C   COSINE TRANSFORM AUTOCORRELATION
C
      DO 30 I=1,NY
      S(I)=0.
      DO 40 K=2,NX
      ARG=3.14159265*FLOAT(I-1)*FLOAT(K-1)/(FLOAT(NY-1))
   40 S(I)=S(I)+A(K)*COS(ARG)
   30 S(I)=A(1)+2.*S(I)
      RETURN
      END
      SUBROUTINE BURG(LX,X,LC,C,EP,EM)
C
C   GIVEN TIME SERIES X(1...LX) GET REFLECTION COEFFICIENTS
C   C(1...LC)
C
      DIMENSION X(1000),EP(1000),EM(1000),C(1000)
      DO 10 I=1,LX
      EM(I)=X(I)
   10 EP(I)=X(I)
      C(1)=-1.
      DO 30 J=2,LC
      DEN=0.



      DPM=0.
      DO 20 I=J,LX
      IMJP1=I-J+1
      DEN=DEN+EP(I)*EP(I)+EM(IMJP1)*EM(IMJP1)
   20 DPM=DPM+EP(I)*EM(IMJP1)
      C(J)=2.*DPM/DEN
      DO 30 I=J,LX
      EPI=EP(I)
      IMJP1=I-J+1
      EP(I)=EP(I)-C(J)*EM(IMJP1)
   30 EM(IMJP1)=EM(IMJP1)-C(J)*EPI
      RETURN
      END
      SUBROUTINE LEVIN(C,NPEF,A)
      REAL C(1000),A(1000)
      A(1)=1.
      DO 10 J=2,NPEF
```

```
      A(J)=0.
      JH=(J+1)/2
      DO 10 I=1,JH
      JMIP1=J-I+1
      BOT=A(JMIP1)-C(J)*A(I)
      A(I)=A(I)-C(J)*A(JMIP1)
   10 A(JMIP1)=BOT
      RETURN
      END
      SUBROUTINE DEPTH(S,DK,DT,D,IP,NFIRST,PERCENT,NX)
      REAL S(1000),D(1000),C(1000)
      DO 1 I=NFIRST,NX
      S(I)=ALOG(S(I))
      IF(S(I).LE.(S(NFIRST)-PERCENT))GO TO 2
1     CONTINUE
2     NMAX=I
      RSUM=0.
      SUM=0.
      CSUM=0.
      SUMI=0.
      M=NMAX-NFIRST+1
      DO 5 I=NFIRST,NMAX
      ARG=1.-EXP(-DT*FLOAT(I-1)*DK)
      C(I)=-ALOG(ARG)+.5*S(I)
      SUM=SUM+FLOAT(I)*C(I)
      CSUM=CSUM+C(I)
      SUMI=SUMI+FLOAT(I)
5     RSUM=RSUM+FLOAT(I)*FLOAT(I)
      D(IP)=(1./DK)*((SUMI*CSUM-FLOAT(M)*SUM)/(FLOAT(M)*RSUM-SUMI*SUMI))
      IP=IP+1
      RETURN
      END
```